sample buffer (62.5 mM Tris–HCl, pH 6.8, 2% sodium laurylsulfate, 10% glycerol, 2.5% β-mercaptoethanol, 0.01% bromophenol blue, 0.005% crystal violet). Western blotting analyses were performed as described previously (Enomoto *et al.*, 2003).

Immunoprecipitation and immune complex kinase assays
Cells were washed in ice-cold phosphate-buffered saline, and then lysed in lysis buffer containing 10 mM Tris–HCl (pH 7.7), 150 mM NaCl, 1% Nonidet P-40, 1 mM EDTA and protease inhibitor mixture (Roche). After centrifugation, the supernatants were incubated with a specific antibody and then mixed with protein A/G agarose. For binding assays, immune complexes were washed three times with lysis buffer, and subjected to western blotting analysis. For immune complex kinase assays, the immunoprecipitates were rinsed three times with lysis buffer and then twice with kinase buffer (12.5 mM Tris–HCl, pH 7.5, 0.025 mM EGTA, 0.025% β-mercaptoethanol, 0.05 mM sodium orthovanadate, 125 μM ATP, 18.75 mM magnesium chloride). For MEKK1/2 kinase assay, the immunoprecipitates were incubated with GST-tagged SEK1 (K129R) in kinase buffer containing 10 μCi ml^{-1} [γ-^{32}P]ATP at 30°C for 15 min. For the analysis of MEKK2 autophosphorylation assay, GST-MEKK2 was incubated with immunopurified STK38 or STK38 (K118A) in kinase buffer containing 10 μCi ml^{-1} [γ-^{32}P]ATP at 30°C for 15 min. The kinase reaction products were subjected to SDS–PAGE and analysed with a phosphoimaging device (BAS-2000; Fuji). For STK38 kinase assay, synthetic peptides (KKRNRRLSVA) were incubated with immunopurified wild-type STK38 or STK38 (K118A) in kinase buffer containing 10 μCi ml^{-1} [γ-^{32}P]ATP at 30°C for 1 h. The kinase reaction products were spotted onto P81 paper disks (Whatman). The disks were washed three times in 1% phosphoric acid before being counted in a liquid scintillation counter.

Plasmid constructions
The open reading frames of mouse STK38, JNK1, SEK1 and MEKK2 were amplified by PCR with reverse transcription using mouse brain total RNA (BD Bioscience) and subcloned into pcDNA3.1-V5, pcDNA4.0-Xpress (Invitrogen), pFLAG-CMV2 (Kodak, Rochester, NY, USA) or pcDNA3-FLAG mammalian expression vectors, respectively. The expression vector for FLAG-tagged MEKK1 was constructed as described (Ito *et al.*, 1999). The amino-terminal region (residues 1–640) of MEKK1 was amplified by PCR and subcloned into pcDNA3-FLAG to generate pcDNA3-FLAG MEKK1N. The region encoding residues 1169–1488 of MEKK1 was amplified by PCR and subcloned into the pEF-HA to generate pEF-HA–ΔMEKK1. The carboxy-terminal regions (residues 342–619 and 425–619) of MEKK2 were amplified by PCR and subcloned into the pcDNA4/His Max expression vector, respectively. The region encoding residues 87–465 of STK38 was amplified by PCR and subcloned into pcDNA3.1-V5 to generate pcDNA3.1ΔN STK38-V5. To generate expression vectors for STK38 (K118A), MEKK2 (K385M) or SEK1 (K129R), site-directed mutagenesis was performed using overlapping PCR methods. The sequences of the open reading frames in the constructed plasmids were confirmed by DNA sequencing.

STK38 small interfering RNA
The pcPURU6βicassette mammalian expression vector (iGene Therapeutics, Tsukuba, Japan) was used for expression of STK38 small interfering RNA. We purchased synthetic oligonucleotides targeting human STK38 (Takara Bio, Ohtsu, Japan), in which sense and antisense nucleotides were connected by an 11-base hairpin loop and formed a single chain. After annealing, the DNA fragments were ligated into the BspMI sites of the pcPURU6βicassette vector. The target sequence was as follows (only the antisense sequence is shown): 5′-AACAAG ACTTGGATTGGAA-3′. HeLa cells were transfected with the control or *stk38*-specific shRNA expression vector using FuGENE HD (Roche). At 24 h after transfection, the medium was replaced with fresh medium containing 0.2 μg ml^{-1} puromycin (InvivoGen, San Diego, CA, USA) for selection of the transformants. Following an additional incubation for 48 h, the cells were treated with various agents, such as 0.2 M sorbitol, and harvested immediately for western blotting analysis.

DNA microarray
Total RNA was prepared from cells using the Ultraspec RNA Isolation System (Biotecx Lab, Houston, TX, USA). Double-stranded cDNA was synthesized from total RNA with a SuperScript Double-Stranded cDNA Synthesis kit (Invitrogen). Biotinylated cRNA was prepared by *in vitro* transcription using a BioArray High Yield RNA Transcript Labeling kit (Enzo, Farmingdale, NY, USA) and then fragmented. For hybridization, the fragmented cRNA was added to a CodeLink Uniset Human 20 K I Bioarray (GE Healthcare, Farmingdale, NY, USA) for 18 h at 37 °C. The bioarrays were stained with Cy5-streptavadin (GE Healthcare, Farmingdale, NY, USA) and scanned using a Gene Pix 4000B scanner (Axon Instruments, Foster City, CA, USA). The spot signals were quantified with ImaGene 5.5 software (BioDiscovery, San Diego, CA, USA).

Acknowledgements

This work was supported in part by grants from the Ministry of Education, Culture, Sport, Science, and Technology, and the Ministry of Health and Welfare of Japan, as well as by the Public Trust Haraguchi Memorial Cancer Research Fund.

References

Bidlingmaier S, Weiss EL, Seidel C, Drubin DG, Snyder M. (2001). The Cbk1p pathway is important for polarized cell growth and cell separation in *Saccharomyces cerevisiae*. *Mol Cell Biol* **21**: 2449 2462.

Blank JL, Gerwins P, Elliott EM, Sather S, Johnson GL. (1996). Molecular cloning of mitogen-activated protein/ERK kinase kinases (MEKK) 2 and 3. Regulation of sequential phosphorylation pathways involving mitogen-activated protein kinase and c-Jun kinase. *J Biol Chem* **271**: 5361 5368.

Cano E, Mahadevan LC. (1995). Parallel signal processing among mammalian MAPKs. *Trends Biochem Sci* **20**: 117 122.

Chang L, Karin M. (2001). Mammalian MAP kinase signaling cascades. *Nature* **410**: 37 40.

Chayama K, Papst PJ, Garrington TP, Pratt JC, Ishizuka T, Webb S *et al.* (2001). Role of MEKK2-MEK5 in the regulation of TNF-alpha gene expression and MEKK2-MKK7 in the activation of c-Jun N-terminal kinase in mast cells. *Proc Natl Acad USA* **98**: 4599 4604.

Chen W, White MA, Cobb MH. (2002). Stimulus-specific requirements for MAP3 kinases in activating the JNK pathway. *J Biol Chem* **277**: 49105 49110.

Cheng J, Yang J, Xia Y, Karin M, Su B. (2000). Synergistic interaction of MEK kinase 2, c-Jun N-terminal kinase (JNK) kinase 2, and JNK1 results in efficient and specific JNK1 activation. *Mol Cell Biol* **20**: 2334 2342.

Cheng J, Yu L, Zhang D, Huang Q, Spencer D, Su B. (2005a). Dimerization through the catalytic domain is essential for MEKK2 activation. *J Biol Chem* **280**: 13477 13482.

Cheng J, Zhang D, Kim K, Zhao Y, Zhao Y, Su B. (2005b). Mip1, an MEKK2-interacting protein, controls MEKK2 dimerization and activation. *Mol Cell Biol* **25**: 5955 5964.

Cobb MH, Goldsmith EJ. (1995). How MAP kinases are regulated. *J Biol Chem* **270**: 14843 14846.

Davis RJ. (2000). Signal transduction by the JNK group of MAP kinases. *Cell* **103**: 239 252.

Deak JC, Templeton DJ. (1997). Regulation of the activity of MEK kinase 1 (MEKK1) by autophosphorylation within the kinase activation domain. *Biochem J* **322**: 185 192.

Enomoto A, Suzuki N, Hirano K, Matsumoto Y, Morita A, Sakai K *et al.* (2000). Involvement of SAPK/JNK pathway in X-ray-induced rapid cell death of human T-cell leukemia cell line MOLT-4. *Cancer lett* **155**: 137 144.

Enomoto A, Suzuki N, Kang Y, Hirano K, Matsumoto Y, Zhu J *et al.* (2003). Decreased c-Myc expression and its involvement in X-ray-induced apoptotic cell death of human T-cell leukemia cell line MOLT-4. *Int J Radiat Biol* **79**: 589 600.

Enslen H, Raingeaud J, Davis RJ. (1998). Selective activation of p38 mitogen-activated protein (MAP) kinase isoforms by the MAP kinase kinase MKK3 and MKK6. *J Biol Chem* **273**: 1741 1748.

Fanger GR, Widmann C, Porter AC, Sather S, Johnson GL, Vaillancourt RR. (1998). 14-3-3 proteins interact with specific MEK kinases. *J Biol Chem* **273**: 3476 3483.

Guo Z, Clydesdale G, Cheng J, Kim K, Gan L, McConkey DJ *et al.* (2002). Disruption of Mekk2 in mice reveals an unexpected role for MEKK2 in modulating T-cell receptor signal transduction. *Mol Cell Biol* **22**: 5761 5768.

Gupta S, Barrett T, Whitmarsh AJ, Cavanagh J, Sluss HK, Derijard B *et al.* (1996). Selective interaction of JNK protein isoforms with transcription factors. *EMBO J* **15**: 2760 2770.

Han J, Lee JD, Bibbs L, Ulevitch RJ. (1994). A MAP kinase targeted by endotoxin and hyperosmolarity in mammalian cell. *Science* **265**: 808 811.

Hergovich A, Stegert MR, Schmitz D, Hemmings BA. (2006). NDR kinases regulate essential cell processes from yeast to humans. *Nat Rev Mol Cell Biol* **7**: 253 264.

Herskowitz I. (1995). MAP kinase pathway in yeast: for mating and more. *Cell* **80**: 187 197.

Ito M, Yoshioka K, Akechi M, Yamashita S, Takamatsu N, Sugiyama K *et al.* (1999). JSAP1, a novel Jun N-terminal protein kinase (JNK)-binding protein that functions as a scaffold factor in the JNK signaling pathway. *Mol Cell Biol* **19**: 7539 7548.

Johnston LH, Eberly SL, Chapman JW, Araki H, Sugino A. (1990). The product of the *Saccharomyces cerevisiae* cell cycle gene *DBF2* has homology with protein kinases and is periodically expressed in the cell cycle. *Mol Cell Biol* **10**: 1358 1366.

Karin M, Ben-Neriah Y. (2000). Phosphorylation meets ubiquitination: the control of NF-κB activity. *Ann Rev Immunol* **18**: 621 663.

Kesavan K, Lobel-Rice K, Sun W, Lapadat R, Webb S, Johnson GL *et al.* (2004). MEKK2 regulates the coordinate activation of ERK5 and JNK in response to FGF-2 in fibroblasts. *J Cell Physiol* **199**: 140 148.

Kyriakis JM, Avruch J. (2001). Mammalian mitogen-activated protein kinase signal transduction pathways activated by stress and inflammation. *Physiol Rev* **81**: 807 869.

Kyriakis JM, Banerjee P, Nikolakaki E, Dai T, Rubie EA, Ahmad MF *et al.* (1994). The stress-activated protein kinase subfamily of c-Jun kinases. *Nature* **369**: 156 160.

Lange-Carter CA, Pleiman CM, Gardner AM, Blumer KJ, Johnson GL. (1993). A divergence in the MAP kinase regulatory network defined by MEK kinase and Raf. *Science* **260**: 315 319.

Lin A, Minden A, Martinetto H, Claret FX, Lange-Carter C, Mercurio F *et al.* (1995). Identification of a dual specificity kinase that activates the Jun kinases and p38-Mpk2. *Science* **268**: 286 290.

Manning G, Plowman GD, Hunter T, Sudarsanam S. (2002). Evolution of protein kinase signaling from yeast to man. *Trends Biochem Sci* **27**: 514 520.

Marshall CJ. (1995). Specificity of receptor tyrosine kinase signaling: transient versus sustained extracellular signal-regulated kinase activation. *Cell* **80**: 179 185.

Minamino T, Yujiri T, Papst PJ, Chan ED, Johnson GL, Terada N. (1999). MEKK1 suppresses oxidative stress-induced apoptosis of embryonic stem cell-derived cardiac myocytes. *Proc Natl Acad USA* **96**: 15127 15132.

Minden A, Lin A, McMahon M, Lange-Carter C, Derijard B, Davis RJ *et al.* (1994). Differential activation of ERK and JNK mitogen-activated protein kinases by Raf-1 and MEKK. *Science* **266**: 1719 1723.

Ryoo K, Huh SH, Lee YH, Yoon KW, Cho SG, Choi EJ. (2004). Negative regulation of MEKK1-induced signaling by glutathione *S*-transferase Mu. *J Biol Chem* **279**: 43589 43594.

Su B, Cheng J, Yang J, Guo Z. (2001). MEKK2 is required for T-cell receptor signals in JNK activation and interleukin-2 gene expression. *J Biol Chem* **276**: 14784 14790.

Tamaskovic R, Bichsel SJ, Hemmings BA. (2003). NDR family of AGC kinases essential regulators of the cell cycle and morphogenesis. *FEBS Lett* **546**: 73 80.

Verde F, Wiley DJ, Nurse P. (1998). Fission yeast *orb6*, a ser/thr protein kinase related to mammalian rho kinase and myotonic dystrophy kinase, is required for maintenance of cell polarity and coordinates cell morphogenesis with the cell cycle. *Proc Natl Acad Sci USA* **95**: 7526 7531.

Waskiewicz AJ, Cooper JA. (1995). Mitogen and stress response pathways: MAP kinase cascades and phosphatase regulation in mammalian and yeast. *Curr Opin Cell Biol* **7**: 798 805.

Xia Y, Wu Z, Su B, Murray B, Karin M. (1998). JNKK1 organizes a MAP kinase module through specific and sequential interactions with upstream and downstream components mediated by its amino-terminal extension. *Genes Dev* **12**: 3369 3381.

Yan M, Dai T, Deak JC, Kyriakis JM, Zon LI, Woodgett JR *et al.* (1994). Activation of stress-activated protein kinase by MEKK1 phosphorylation of its activator SEK1. *Nature* **372**: 798 800.

Yang J, Lin Y, Guo Z, Cheng J, Huang J, Deng L *et al.* (2001). The essential role of MEKK3 in TNF-induced NF-κB activation. *Nat Immunol* **2**: 620 624.

Yujiri T, Ware M, Widmann C, Oyer R, Russell D, Chan E *et al.* (2000). MEK kinase 1 gene disruption alters cell migration and c-Jun NH_2-terminal kinase regulation but does not cause a measurable defect in NF-κB activation. *Proc Natl Acad USA* **97**: 7272 7277.

Zhang D, Facchinetti V, Wang X, Huang Q, Qin J, Su B. (2006). Identification of MEKK2/3 serine phosphorylation site targeted by the Toll-like receptor and stress pathways. *EMBO J* **25**: 97 107.

Supplementary Information accompanies the paper on the Oncogene website (http://www.nature.com/onc)

J. Radiat. Res., 48, 495–503 (2007) Regular Paper

Free Radical Scavenger Edaravone Suppresses X-ray-induced Apoptosis through p53 Inhibition in MOLT-4 Cells

Nakashi SASANO[1,2], Atsushi ENOMOTO[2], Yoshio HOSOI[2], Yosuke KATSUMURA[3], Yoshihisa MATSUMOTO[2], Kenshiro SHIRAISHI[1], Kiyoshi MIYAGAWA[2], Hiroshi IGAKI [1] and Keiichi NAKAGAWA[1]*

X-ray-induced apoptosis/Edaravone/MOLT-4 cells/Radioprotective effect/Free radical scavenger.

Edaravone, a clinical drug used widely for the treatment of acute cerebral infarction, is reported to scavenge free radicals. In the present study, we investigated the radioprotective effect of edaravone on X-ray-induced apoptosis in MOLT-4 cells. Apoptosis was determined by the dye exclusion test, Annexin V binding assay, cleavage of caspase, and DNA fragmentation. We found that edaravone significantly suppressed the X-ray-induced apoptosis. The amount of intracellular ROS production was determined by the chloromethyl-2',7'-dichlorodihydro-fluorescein diacetate system. We found that the intracellular ROS production by X-irradiation was completely suppressed by the addition of edaravone. The accumulation and phosphorylation of p53 and the expression of $p21^{WAF1}$, a target protein of p53, which were induced by X-irradiation, were also suppressed by adding edaravone. We conclude that the free radical scavenger edaravone suppresses X-ray-induced apoptosis in MOLT-4 cells by inhibiting p53.

INTRODUCTION

X-ray-induced cell death results from two types of actions, direct and indirect.[1)] In the first, the X-rays directly ionize or excite macromolecules in the cells, leading to cell damage. In the second, the X-rays excite water molecules in the cells and produce reactive oxygen species (ROS), which damage the cells. Approximately 70% of the biological damage caused by X-rays results from this indirect action.[2)] Cells that are critically damaged by X-rays will die either by interphase cell death or reproductive cell death.[3)] Most of the X-ray-induced cell deaths observed in thymocytes are of the interphase type, known as apoptosis.[4,5)] ROS are postulated to play a central role in X-ray-induced apoptosis,[6)] with the hydroxyl radical being the most important. Thus, agents that could suppress ROS would be expected to protect cells from X-ray-induced apoptosis and improve cell survival.

Edaravone (MCI-186; 3-methyl-1-phenyl-2-pyrazolin-5-one; Radicut) is a clinical drug that is used widely for the treatment of acute cerebral infarction. Its effectiveness as a treatment for this condition has been reported in many studies, including *in vivo*,[7–20)] *in vitro*,[21,22)] and clinical settings.[23–26)] Edaravone scavenges free radicals as an electron donor[27–29)]; therefore, it seemed likely to be useful for radioprotection.

Indeed, in a previous study, Anzai and colleagues reported that the intraperitoneal administration of edaravone to mice increased the lethal dose of radiation for the animals,[30)] indicating that the drug has a radioprotective effect. In that report, edaravone's radioprotective effect was probably due mainly to the suppression of bone-marrow syndrome, because the X-ray dose used in the experiment was under 10 Gy.[30)] However, edaravone's radioprotective mechanism is not fully understood at the molecular level.

Bone-marrow syndrome occurs mainly as a result of the apoptosis of stem cells.[31)] In the present study, we investigated the effect of edaravone on the apoptosis of MOLT-4 cells after X-irradiation. The human T-cell leukemia cell line MOLT-4 is highly sensitive to X-rays; after X-irradiation it undergoes an apoptotic cell death that is characterized by nuclear condensation and DNA fragmentation and is mediated by activated caspases.[32–35)] Recent studies have demonstrated that the p53 and JNK pathways are involved in the radiation-induced apoptosis of MOLT-4 cells.[34–37)] The results presented here suggest that edaravone suppresses the X-ray-induced apoptosis in MOLT-4 cells by inhibiting p53 and caspase.

*Corresponding author: Phone: +81-3-3815-5411,
Fax: +81-3-5800-8935,
E-mail: nakagawa-rad@umin.ac.jp
[1]Department of Radiology, Graduate School of Medicine, The University of Tokyo; [2]Section of Radiation Biology, Center for Disease Biology and Integrative Medicine, Faculty of Medicine, The University of Tokyo; [3]Nuclear Engineering Research Laboratory, Graduate School of Engineering, The University of Tokyo.
doi:10.1269/jrr.07061

MATERIALS AND METHODS

Cell culture

Human T-cell leukemia MOLT-4 cells were cultured in suspension with RPMI-1640 medium (Sigma) containing 5% fetal bovine serum (Hyclone) and antibiotics (100 units/ml of penicillin/streptomycin), and incubated at 37°C in a humidified atmosphere of 5% CO_2 and 95% air.

Chemicals

Edaravone was kindly provided by the Mitsubishi Pharma Corporation (Tokyo, Japan). We dissolved 52.5 mg edaravone in 192.5 μl of 2 M NaOH and 1.05 ml of DDW, and then adjusted the pH to 8.8 with 2 M HCl. Finally, physiological saline was added to adjust the final concentration of edaravone to 30 mg/ml.

X-irradiation

X-irradiation was performed with an X-ray generator (Pantak HF 350, Shimadzu) at 200 kVp and 20 mA, with a filter of 0.5 mm Cu and 1 mm Al, and at a dose rate of 1.35–1.40 Gy/min.

Dye exclusion test

One hundred microliters of cell suspension (approximately 5×10^5 cells/ml) was mixed with 25 μl of 1% erythrosin B in phosphate-buffered saline (PBS). The numbers of stained (dead) cells and unstained (live) cells were counted and the viability (%) was calculated as follows:

Viability (%) = (number of unstained cells/ total cell number) × 100

Annexin V Binding Assay

The extent of apoptosis was determined by Annexin V-FITC and propidium iodine (PI) staining, using the MEBCYTO Apoptosis Kit (MBL). Flow cytometric analysis was carried out with an EPICS flow cytometer (XL System II, Beckman Coulter), using a single laser emitting excitation light at 488 nm. In the FITC/PI diparametric plot, quadrants 1 (lower FITC/ upper PI), 2 (upper FITC/ upper PI), 3 (lower FITC/ lower PI), and 4 (upper FITC/ lower PI) represent the fractions of secondary-necrotic, primary-necrotic, viable, and apoptotic cells, respectively. More than 5,000 cells were subjected to the analysis.

Quantification of intracellular ROS

The amount of intracellular ROS production was measured by chloromethyl-2', 7'-dichlorodihydro-fluorescein diacetate (CM-H_2-DCFDA, Molecular Probes). MOLT-4 cells were incubated in the dark with approximately 5 μg/ml of probe CM-H_2-DCFDA for an hour, and the fluorescence intensity was analyzed by an EPICS flow cytometer (XL System II, Beckman Coulter) using a laser excitation and emission wavelength of 492–495 nm and 517–527 nm, respectively.

Western blot analysis

Cells were lysed in a sodium dodecyl sulfate (SDS) sample buffer (1% SDS, 3% β-mercaptoethanol, 5% glycerol, 62.5 mM, Tris-HCl, pH 6.8). Proteins were separated by 10% or 15% SDS-polyacrylamide gel electrophoresis (SDS-PAGE) and were transferred onto polyvinylidene difluoride membranes (Immobilon, Millipore). After blocking for 30

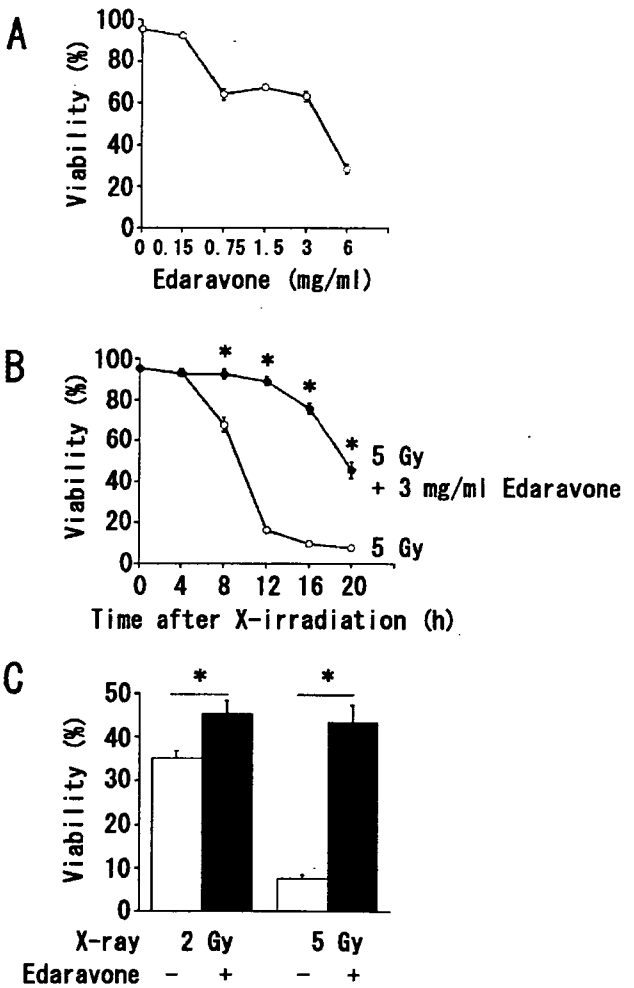

Fig. 1. Cell viabilities were determined by dye exclusion test using erythrosin B. (A) The toxicity of edaravone was examined at various concentrations. Cell viability was determined 20 hours after edaravone administration. (B) Time course of cell viability after X-irradiation. MOLT-4 cells were untreated or treated with 3 mg/ml edaravone, then subjected to 5 Gy X-irradiation 5 minutes later. (C) Effects of radiation dose on cell viability. MOLT-4 cells were irradiated at 2 or 5 Gy with or without edaravone pretreatment as in B, and the cell viability was determined 20 hours later. Data shown are means ± SD from at least three independent experiments. *$p < 0.05$.

minutes in 5% skim milk in Tris-buffered saline (TBS, 29 mM Tris-HCl, 0.9% NaCl, pH 7.6) supplemented with 0.05% Tween-20 (TBS-T), the membranes were incubated overnight at 4°C in TBS-T containing 5% skim milk and primary antibodies. The primary antibodies were anti-p53 (clone DO-1, Santa Cruz Biotechnology), anti-phospho p53 at Ser 15 (Calbiochem), anti-cleaved caspase-3 (Cell Signaling), anti-caspase-7 (MBL), anti- $p21^{WAF1}$ (Calbiochem), and anti-Bcl-2 (Pharmingen). After being rinsed with TBS-T three times, the membranes were incubated overnight at 4°C in TBS-T containing 5% skim milk and secondary antibodies conjugated with horseradish peroxidase (DAKO). The membranes were then washed three times with TBS-T, once with TBS (20 mM Tris-HCl, pH 7.5, 150 mM NaCl), and developed using an ECL-plus kit (Amersham Biosciences). The signals were obtained by exposure to X-ray

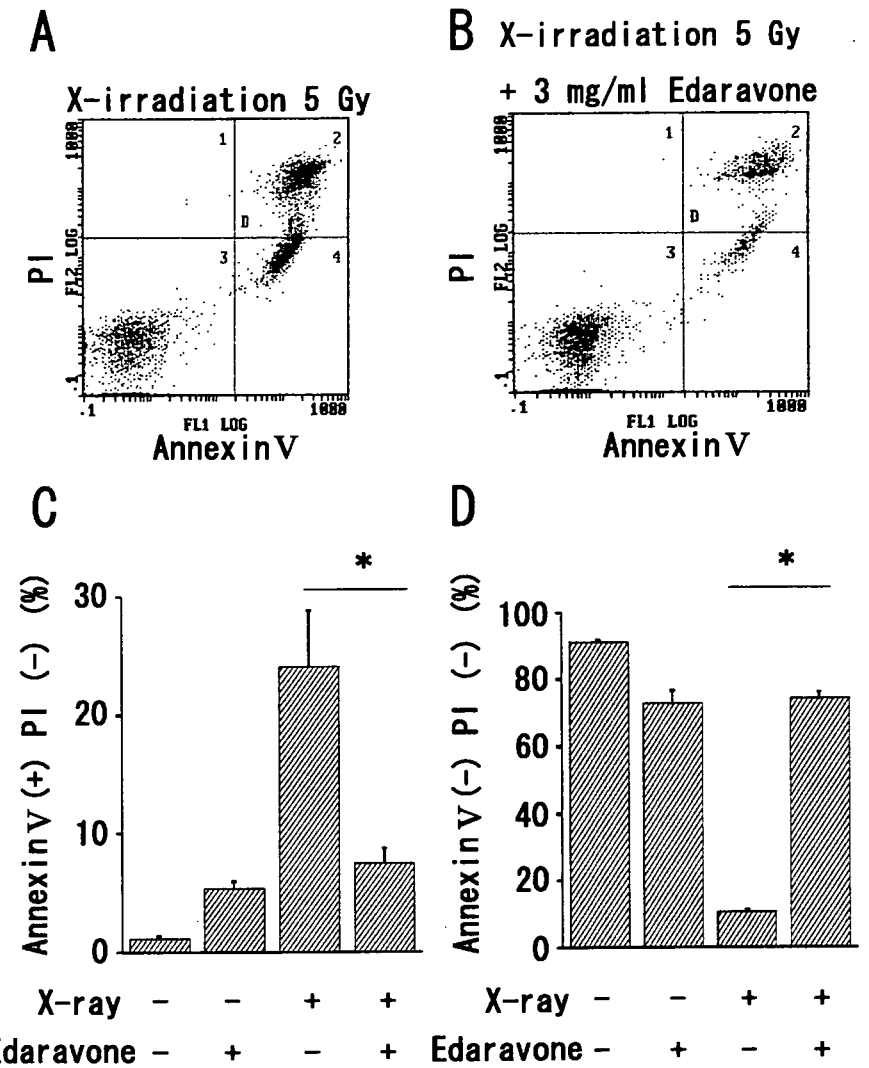

Fig. 2. Effect of edaravone on apoptosis, determined by Annexin V- PI staining. (A) MOLT-4 cells were subjected to 5 Gy X-irradiation without edaravone treatment. (B) MOLT-4 cells were subjected to 5 Gy X-irradiation 5 minutes after the addition of 3 mg/ml edaravone. Typical flow cytometry results of Annexin V- PI staining performed 16 hours after X-irradiation are shown. The transverse axis shows Annexin V -stained cells and the vertical axis shows PI-stained cells. (C) The percentage of cells stained by Annexin V and unstained by PI, which is interpreted as in the early stage of apoptosis, is shown. MOLT-4 cells were harvested 16 hours after treatment (5 Gy X-irradiation and/or 3 mg/ml edaravone 5 minutes before X-irradiation). (D) The percentage of cells unstained both by Annexin V and PI is shown. MOLT-4 cells were harvested 20 hours after treatment (5 Gy X-irradiation and/or 3 mg/ml edaravone 5 minutes before X-irradiation). *$p < 0.05$.

films (Hyperfilm MP, Amersham Biosciences).

Analysis of DNA fragmentation

Approximately 1×10^6 of control or treated cells were harvested at the indicated time points. DNA was extracted using the Apoptosis Ladder Detection Kit (WAKO), according to the manufacturer's instructions. The DNA pellet was washed, resuspended, and subjected to electrophoresis on a 1.5% agarose gel at 100 volts for 30 minutes. The gel was visualized by staining with 1 μg/ml ethidium bromide and observed under a UV transilluminator and photographed.

Statistical analysis

All experiments were repeated at least three times. The results are expressed as the mean ± standard deviation (SD) of the mean. All laboratory data were evaluated according to standard statistical methods, using commercially available computer programs such as Microsoft Excel 2000. Statistical differences were determined using the Student's *t*-test. In all tests, p values less than 0.05 were considered statistically significant.

RESULTS

Effects of edaravone on X-ray-induced cell death

First, to determine the optimal concentration of edaravone to use in the experiments, we investigated its cytotoxicity using the dye exclusion test. The cell viability was examined in cultures treated with 0.15, 0.75, 1.5, 3, and 6 mg/ml edaravone (Fig. 1A). At concentrations of edaravone less than 3 mg/ml, the cell viability was more than approximately 60%, which was considered acceptable. A dose of 6 mg/ml, however, proved cytotoxic for MOLT-4 cells (Fig. 1A). Thus, we performed the following experiments using a concentration of 3 mg/ml.

To examine the effects of edaravone on X-ray-induced cell death, we determined the time course of cell viability after 5 Gy X-irradiation with or without 3 mg/ml edaravone, using the dye exclusion test. When MOLT-4 cells were irradiated without edaravone, the cell viability 4, 8, 12, 16, and 20 hours after X-irradiation was 93.3 ± 1.7%, 67.8 ± 3.4%, 16.5 ± 1.2%, 9.6 ± 1.4%, and 7.7 ± 0.8%, respectively (Fig. 1B). When edaravone was added 5 minutes before the X-irradiation, the cell viability was 92.8 ± 1.4%, 92.6 ± 2.4%, 89.2 ± 2.0%, 75.8 ± 2.6%, and 45.6 ± 4.1%, respectively (Fig. 1B). The cell viability with edaravone was significantly higher from 8 to 20 hours after X-irradiation than that of cells that were not treated with edaravone ($p < 0.05$). These data indicate that edaravone significantly inhibited the X-ray-induced cell death of MOLT-4 cells. We also performed the same examination with 1.5 mg/ml edaravone, however, the cell viability did not increase significantly when 1.5 mg/ml edaravone was added 5 minutes before X-irradiation (data not shown).We considered that less than 1.5 mg/ml edaravone had no effect on the MOLT-4 cell viability after X-irradiation.

Next, we examined the effect of the radiation dose on the cell viability after X-irradiation. MOLT-4 cells were untreated or treated with 3 mg/ml edaravone, then subjected to 2 or 5 Gy X-irradiation 5 minutes later. The dye exclusion test was performed 20 hours after X-irradiation. The cell viability after 2 and 5 Gy X-irradiation without edaravone was 36.7 ± 1.7% and 7.7 ± 0.8%, respectively (Fig. 1C). The cell viability after 2 and 5 Gy X-irradiation with edaravone treatment was 45.5 ± 2.9% and 45.6 ± 4.1%, respectively (Fig. 1C). The cell viability at X-ray doses of 2 and 5 Gy was significantly improved by the addition of edaravone ($p < 0.05$).

Next, we examined the effect of the edaravone added after X-irradiation on the cell viability. MOLT-4 cells were subjected to 5 Gy X-irradiation, then untreated or treated with 3 mg/ml edaravone 4 hours later. The dye exclusion test was performed 20 hours after X-irradiation. The cell viability was partially improved when edaravone was added 4 hours after X-irradiation (data not shown).

Effects of edaravone on apoptosis

To assess the effect of edaravone on X-ray-induced apoptosis, we performed Annexin V-PI staining 16 or 20 hours after X-irradiation by flow cytometry. The appearance of Annexin V+/PI– cells, which were interpreted as in the early stage of apoptosis, was significantly suppressed by the addition of 3 mg/ml edaravone 5 minutes before X-irradiation ($p < 0.05$) (Fig. 2A–C). The percentage of Annexin V–/PI– cells, which were interpreted as viable, was 10.6 ± 0.8% when the cells were irradiated without 3 mg/ml edaravone

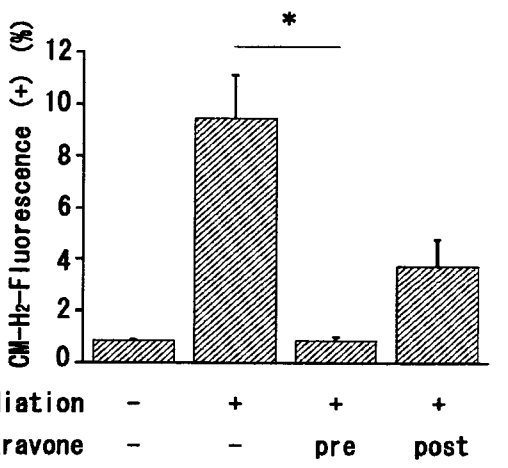

Fig. 3. Intracellular ROS determined by the CM-H_2-DCFDA flow cytometry system. The amount of intracellular ROS after treatment (20 Gy X-irradiation with or without 3 mg/ml edaravone) is shown. Edaravone was added 5 minutes before or after X-irradiation. The ROS production of each sample was quantified as described in Materials and Methods. Data shown are means + SD from at least three independent experiments. *$p < 0.05$.

and 74.2 ± 2.1% when they were X-irradiated with edaravone ($p < 0.05$) (Fig. 2D). These data indicate that the radioprotective effect of edaravone is due to the suppression of apoptosis.

We also examined the effect of 3 mg/ml edaravone added 4 hours after X-irradiation on X-ray-induced apoptosis. Annexin V-PI staining was performed 16 hours after 5 Gy-X-irradiation. The appearance of Annexin V+/PI– cells was partially suppressed by the addition of 3 mg/ml edaravone 4 hours after X-irradiation (data not shown).

Effects of edaravone on the production of intracellular ROS

To examine the effect of edaravone on the X-ray-induced production of intracellular ROS, we used the CM-H_2-DCFDA flow cytometry system.[38] CM-H_2-DCFDA is a fluorescence-based probe that was recently developed to detect the intracellular production of ROS. CM-H_2-DCFDA

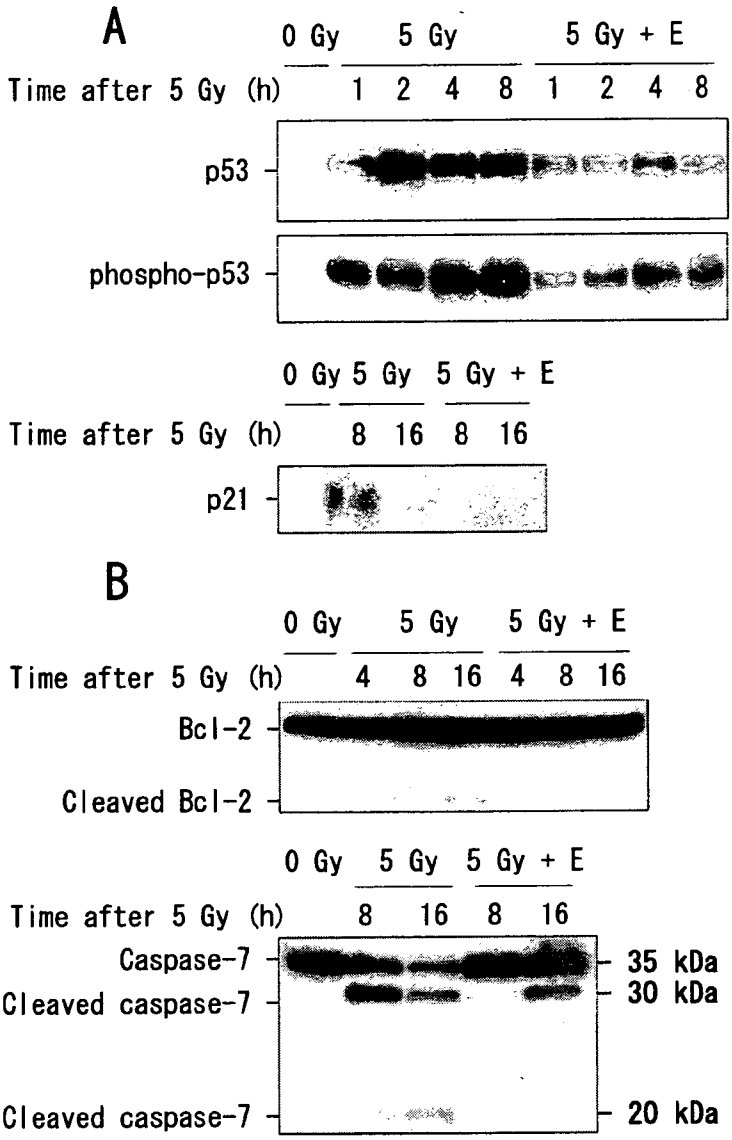

Fig. 4. Time course of the effects of edaravone (E) on apoptosis-related proteins. MOLT-4 cells were untreated or treated with 3 mg/ml edaravone, then subjected to X-irradiation at 5 Gy 5 minutes later. Proteins were detected by immunoblotting. (A) Effects of edaravone on the accumulation and phosphorylation on Ser 15 of p53 and the induction of $p21^{WAF1}$, a p53 target gene, after X-irradiation. (B) Effects of edaravone on apoptosis-related proteins Bcl-2 and caspase-7.

diffuses passively into cells, is trapped inside, and is deacetylated by intracellular esterases. It is subsequently oxidized to a fluorescent product in the presence of intracellular ROS. The oxidation of CM-H_2-DCFDA can be monitored as a convenient determinant of the level of intracellular oxidative stress. X-irradiation at 20 Gy induced an approximately 11-fold increase in basal CM-H_2-DCFDA fluorescence ($p < 0.05$), which was completely suppressed by adding 3 mg/ml edaravone 5 minutes before X-irradiation (Fig. 3). When 3 mg/ml edaravone was added 5 minutes after X-irradiation, however, the basal CM-H_2-DCFDA fluorescence did not decrease significantly (Fig. 3). These data suggest that edaravone eliminates the short-term intracellular ROS generated by X-irradiation.

Effects of edaravone on apoptosis-related proteins

We next investigated the effect of edaravone on the accumulation of p53 and on the phosphorylation of p53 at Ser 15 after X-irradiation, by immunoblotting. Fig. 4A shows that both the accumulation of p53 and its phosphorylation at Ser 15 were apparent 1 hour after X-irradiation, and both were suppressed by 3 mg/ml edaravone. Next, we investigated the expression of the p53 target gene, $p21^{WAF1}$. The expression of $p21^{WAF1}$ was apparent 8 hours after X-irradiation, and this expression was inhibited by 3 mg/ml edaravone (Fig. 4A).

We further investigated the effect of edaravone on caspase-3, caspase-7, and Bcl-2 after X-irradiation. The cleavage of caspase-3 was detectable 8 hours after X-irradiation, and this induction was almost completely suppressed by adding 3 mg/ml edaravone (data not shown). The cleavage of caspase-7 induced by X-irradiation was also suppressed by the addition of 3 mg/ml edaravone (Fig. 4B). On the other hand, Bcl-2, which is a known anti-apoptotic protein, was not overexpressed in response to edaravone addition, suggesting that Bcl-2 might not be responsible for the inhibition of apoptosis by edaravone. The cleavage of Bcl-2 was induced 16 hours after X-irradiation, and this cleavage was suppressed by edaravone addition (Fig. 4B), consistent with Bcl-2's status as a substrate molecule for caspase-3. These data indicate that the addition of edaravone before X-irradiation affects the p53 pathway and caspase activation, but not Bcl-2 overexpression.

Effects of edaravone on DNA fragmentation

DNA fragmentation is a hallmark of apoptosis.[39] It is induced by the activation of caspases, including caspase-3.[39] We examined the effect of edaravone on DNA fragmentation in MOLT-4 cells after X-irradiation. DNA fragmentation was detectable 8 hours after irradiation, and was almost completely suppressed by the addition of 3 mg/ml edaravone (Fig. 5), confirming that the activation of caspase was suppressed by edaravone. The electrophoretic pattern of DNA extracted from MOLT-4 cells irradiated with 5 Gy without addition of edaravone showed a smear pattern, not a ladder pattern, which is compatible with the observation of Akagi and colleagues.[40]

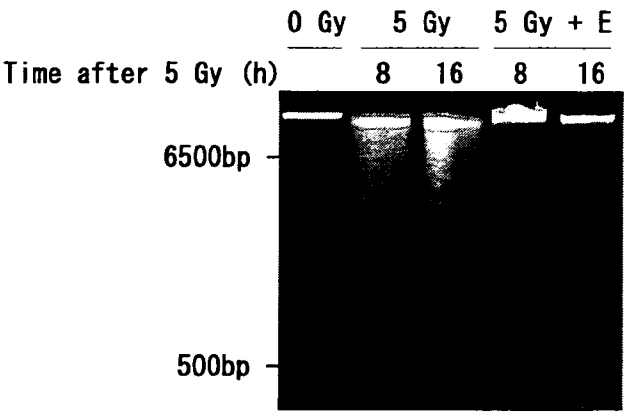

Fig. 5. Effects of edaravone (E) on the DNA fragmentation of irradiated MOLT-4 cells. Cells were untreated or treated with 3 mg/ml edaravone, then subjected to 5 Gy X-irradiation 5 minutes later. The cells were harvested 8 or 16 hours after X-irradiation and analyzed for DNA fragmentation by agarose gel electrophoresis.

DISCUSSION

We found that edaravone suppressed X-ray-induced cell death *in vitro* (Fig. 1). This finding is consistent with the results of a previous *in vivo* study, in which the lethal dose of X-irradiation for mice increased after the administration of edaravone.[30] In addition, we found that this radioprotective effect is due to the suppression of apoptosis (Fig. 2). Previous reports indicated that ROS play a crucial role in the induction of apoptosis.[41,42] We therefore investigated the amount of ROS after X-irradiation with or without edaravone addition, and found that the ROS were significantly suppressed when edaravone was added 5 minutes before X-irradiation, whereas the suppression was not significant when the drug was added 5 minutes after X-irradiation (Fig. 3). This result supports the previous finding that edaravone added after X-irradiation is ineffective as a radioprotector *in vivo*.[30] Edaravone, which exists as an anion in solution, provides an electron to ROS generated by X-irradiation and inactivates them.[27–29] One of the most important ROS is the hydroxyl radical, which reacts with biological components immediately upon being generated, and diminishes soon thereafter. Adding edaravone 5 minutes after X-irradiation might be too late to scavenge hydroxyl radicals generated by the X-irradiation, which could explain its lack of effectiveness at this time point. We propose that edaravone suppresses X-ray-induced apoptosis mainly by scavenging ROS. However, X-ray-induced apoptosis was partially suppressed even when edaravone was added 4 hours after X-irradiation. Other mechanisms may be related to the suppression of apoptosis, however, and further investigation is needed.

p53 is a transcription factor that is well-known to be involved with the cell's decision between apoptosis and other fates after X-irradiation. After DNA damage, p53's stability is increased by phosphorylation,[36] and the accumulated p53 induces the transcription of its target genes,[43] one of which is a cyclin kinase inhibitor, $p21^{WAF1}$.[44] The overexpression of a dominant-negative form of p53 in MOLT-4 cells results in a resistance of the cells to radiation-induced apoptosis.[31] We found that edaravone suppressed the X-ray-induced accumulation of p53 and its phosphorylation at Ser 15 (Fig. 4A). The expression of $p21^{WAF1}$ after X-irradiation was also suppressed by edaravone, confirming that it inhibited the X-ray-induced p53 activation (Fig. 4A).

Caspases are a family of aspartate-specific cysteine proteases that are activated during apoptosis. They are normally present in cells as proenzymes and require limited proteolysis for activation of their enzymatic activity. Activated caspases precipitate the irreversible commitment of the cell to apoptotic death by cleaving a number of substrates, one of which is Bcl-2.[45–47] Bcl-2 is an integral membrane protein that inhibits the apoptosis induced by various stimuli, including heat shock, serum depletion, and chemotherapy agents.[48] We previously reported that MOLT-4 cells transfected with mouse Bcl-2 (MOLT-4/ mbcl-2) are resistant to X-rays; that is, X-ray-induced apoptosis/rapid cell death was significantly suppressed in the Bcl-2-transfected cells.[34] It is reported that the loop domain of Bcl-2 is cleaved at Asp 34 by caspase-3 *in vitro*, and the carboxyl-terminal Bcl-2 cleavage product is pro-apoptotic.[49] In this study, the cleavage of caspase-3 and caspase-7 induced by X-irradiation was suppressed by the prior addition of edaravone (data not shown, Fig. 4B). The findings that edaravone suppresses the activation of p53 and the cleavage of caspase-3 and caspase-7 could be explained by its suppression of ROS. In contrast, the expression of Bcl-2, an anti-apoptotic protein, did not change with the addition of edaravone before X-irradiation (Fig. 4B). This observation is inconsistent with some previous reports, in which the expression of Bcl-2 was increased by edaravone in cerebral ischemic models *in vivo*[15,50] and *in vitro*.[51] The discrepancy between the present results and those of previous studies *in vivo*[15,50] might be related to differences between the *in vitro* and *in vivo* conditions. The discrepancy may also be due to differences in the genetic background of the cells used, MOLT-4 vs. PC12, and/or in the apoptotic stimuli used, X-rays vs. oxygen-glucose deprivation.[51] Another previous report suggested that the X-ray-induced apoptosis in MOLT-4 cells is fully p53-dependent.[32]

Several compounds have been shown to protect living cells from the deleterious effects of X-irradiation. The reported mechanisms of radioprotection, however, differ from compound to compound. For instance, vanadate directly suppresses p53 transactivation,[45] although its affect on ROS has not been investigated. Various antioxidants, including alpha lipoic acid or carboxycysteine-lysine salt, amifostine, reduced glutathione, and vitamin A plus vitamin E plus Vitamin C, all suppressed ROS *in vivo*.[52] Inanami and colleagues reported that a vitamin E analogue, Trolox, which is reported to inhibit lipid peroxidation,[53] suppresses the X-ray-induced apoptosis of MOLT-4 cells by inhibiting the caspase-3-dependent pathway.[54] Edaravone is also reported to inhibit lipid peroxidation,[11,19,55,56] and we found here that it suppressed p53 and caspase activation. Amifostine is a clinical drug with cytoprotective activity against the adverse effects of radiotherapy and chemotherapy in normal tissues; this cytoprotection is attributed to its radioprotective ability to scavenge free radicals[57] and to its antimutagenic effects.[58] These similar and dissimilar mechanisms of the suppression of apoptosis by various agents are still controversial.

Taking our findings together, we conclude that edaravone scavenges ROS generated by X-irradiation, which suppresses the activation of the p53- and caspase- mediated apoptotic pathway and of DNA fragmentation, and, thus, suppresses X-irradiation-induced apoptosis. Since malignant tumors often are hypoxic, edaravone might protect only normal tissues, not malignant tumors, from X-ray-induced cell damage in radiation therapy.

ACKNOWLEDGEMENTS

We thank all the members of our laboratory for their help and encouragement. We also thank Dr. T. Kondo (University of Toyama) for various suggestions and instructions, especially regarding the measurement of the amount of intracellular ROS. This study was supported, in part, by Mitsubishi Pharma Corporation (Tokyo, Japan).

REFERENCES

1. Bernhard, W. A. and Close, D. M. (2004) Charged Particle and Photon Interaction with Matter. Eds. Mozunder, A. and Hatano, Y., pp. 431–470, Marcel Dekker Inc.
2. von Sontag, C. (1987) The Chemical Basis of Radiation Biology. Tayler and Fransis, New York.
3. Radford, I. R. and Murphy, T. K. (1994) Radiation response of mouse lymphoid and myeloid cell lines: III. Different signals can lead to apoptosis and may influence sensitivity to killing by DNA double-strand breakage. Int. J. Radiat. Biol. **65**: 229–239.
4. Kerr, J. F. R., Wyllie, A. H. and Currie, A. R. (1972) Apoptosis: a basic biological phenomenon with wide range implications in tissue kinetics. Br. J. Cancer **26**: 239–257.
5. Yamada, T. and Ohyama, H. (1988) Radiation-induced interphase death of rat thymocyte is internally programmed (apoptosis). Int. J. Radiat. Biol. **53**: 65–75.
6. Hosokawa, Y., Tanaka, L., Kaneko, M., Sakakura, Y., Tsuruga, E., Irie, K. and Yajima, T. (2002) Apoptosis induced by generated OH radicals inside cells after irradiation. Arch. Histol. Cytol **65**: 301–305.
7. Watanabe, T., Yuki, S., Egawa, M. and Nishi, H. (1994) Pro-

tective effects of MCI-186 on cerebral ischemia: Possible involvement of free radical scavenging and antioxidant actions. J. Pharmacol. Exp. Ther. **268**: 1597–1603.
8. Yamamoto, T., Yuki, S., Watanabe, T., Mitsuka, M., Saito, K. and Kogure, K. (1997) Delayed neuronal death prevented by inhibition of hydroxyl radical formation in a transient cerebral ischemia. Brain Res. **762**: 240–242.
9. Mizuno, A., Uemura, K. and Nakashima, M. (1998) Inhibitory effect of MCI-186, a free radical scavenger, on cerebral ischemia following rat middle cerebral artery occlusion. Gen. Parmacol. **30**: 575–578.
10. Abe, K., Yuki, S. and Kogure, K. (1988) Strong attenuation of ischemic and postischemic brain edema in rats by a novel free radical scavenger. Stroke **19**: 280–285.
11. Nishi, H., Watanabe, T., Sakurai, H., Yuki, S. and Ishibashi, A. (1989) Effect of MCI-186 on brain edema in rats. Stroke **20**: 1236–1240.
12. Watanabe, T. and Egawa, M. (1994) Effects of an antistroke agent MCI-186 on cerebral arachidonate cascade. J. Pharmacol. Exp. Ther. **271**: 1624–1629.
13. Kawai, H., Nakai, H., Suga, M., Yuki, S., Watanabe, T. and Saito, K. -I. (1997) Effects of a novel free radical scavenger, MCI-186, on ischemic brain damage in the rat distal middle cerebral artery occlusion model. J. Pharmacol. Exp. Ther. **281**: 921–927.
14. Watanabe, K., Watanabe, K., Kuwahara, T. and Yamamoto, Y. (1997) Free radical-induced oxidation products of 3-methyl-1-phenyl-2-pyrazolin-5-one (MCI-186). J. Jpn. Oil Chem. Soc. **46**: 797–801.
15. Amemiya, S., Kamiya, Y., Nito, C., Inaba, Y., Kato, K., Ueda, M., Shimazaki, K. and Katayama, Y. (2005) Anti-apoptotic and neuroprotective effects of edaravone following focal ischemia in rats. Eur. J. Pharmacol. **516**: 125–130.
16. Shichinohe, Y., Kuroda, S., Yasuda, H., Ishikawa, T., Iwai, M., Horiuchi, M. and Iwasaki, Y. (2004) Neuroprotective effects of the free radical scavenger Edaravone (MCI-186) in mice permanent focal brain ischemia. Brain Res. **1029**: 200–206.
17. Nito, C., Kamiya, T., Amemiya, S., Kato, K. and Katayama, Y. (2003) The neuroprotective effect of a free radical scavenger and mild hypothermia following transient focal ischemia in rats. Acta. Neurochir. Suppl. **86**: 199–203.
18. Ikeda, T., Xia, XY., Kaneko, M., Sameshima, H. and Ikenoue, T. (2002) Effect of the free radical scavenger, 3-methyl-1-phenyl-2-pyrazolin-5-one (MCI-186), on hypoxia-ischemia-induced brain injury in neonatal rats. Neurosci. Lett. **329**: 33–36.
19. Noor, JI., Ikeda, T., Ueda, Y. and Ikenoue, T. (2005) A free radical scavenger, edaravone, inhibits lipid peroxidation and the production of nitric oxide in hypoxic-ischemic brain damage of neonatal rats. Am. J. Obstet. Gynecol. **193**: 1703–1708.
20. Nakashima, N., Niwa, M., Iwai, T. and Uematsu, T. (1999) Involvement of free radicals in cerebral vascular reperfusion injury evaluated in a transient focal cerebral ischemia model of rat. Free Radic. Biol. Med. **26**: 722–729.
21. Watanabe, T., Morita, I., Nishi, H. and Murota, S. (1988) Preventive effect of MCI-186 on 15-HPETE induced vascular endothelial cell injury *in vitro*. Prostaglandins Leukot. Essent. Fatty Acids **33**: 81–87.
22. Yamaguchi, T., Ida, T., Kobayashi, T., Hiraga, M., Oishi, K., Uchida, M. K. and Echizen, H. (2004) Alterations of antiproliferative effects of serum obtained from patients with acute cerebral infarction treated with a radical scavenger, edaravone, with or without amlodipine using an *in vitro* cultured basilar artery smooth muscle cells. Yakugaku Zasshi **124**: 25–29.
23. Edaravone Acute Infarction Study Group. (2003) Effect of a novel free radical scavenger, edaravone (MCI-186), on acute brain infarction. Randomized placebo-controlled, double-blind study at multicenters. Cerebrovasc Dis. **15**: 222–229.
24. Toyoda, K., Fujii, K., Kamouchi, M., Nakane, H., Arihiro, S., Okada, Y., Ibayashi, S. and Iida, M. (2004) Free radical scavenger, edaravone, in stroke with internal carotid artery occlusion. J. Neurol. Sci. **221**: 11–17.
25. Watanabe, T., Tanaka, M., Watanabe, K., Takamatsu, Y. and Tobe, A. (2004) Research and development of the free radical scavenger edaravone as a neuroprotectant. Yakugaku Zasshi. **124**: 99–111.
26. Mishina, M., Komaba, Y., Kobayashi, S., Tanaka, N., Kominami, S., Fukuchi, Y., Mizunari, T., Hamamoto, M., Teramoto, A. and Katayama, Y. (2005) Efficacy of edaravone, a free radical scavenger, for the treatment of acute lacunar infarction. Neurol. Med. Chir. (Tokyo) **45**: 344–348. discussion 348.
27. Watanabe, K., Watanabe, K. and Hayase, T. (1997) Radical scavenging mechanism of MCI-186. Jpn. Pharmacol. Ther. **25**: S1699–S1707.
28. Watanabe, K., Watanabe, K., Kuwahara, T. and Yamamoto, Y. (1997) Free radical-induced oxidation products of 3-methyl-1-phenyl-2-pyrazolin-5-one (MCI-186). J. Jpn. Oil. Chem. Soc. **46**: 797–801.
29. Abe, S., Kirima, K., Tsuchiya, K., Okamoto, M., Hasegawa, T., Houchi, H., Yoshizumi, M. and Tamaki, T. (2004) The reaction rate of edaravone (3-methyl-1-phenyl-2-pyrazolin-5-one (MCI-186)) with hydroxyl radical. Chem. Pharm. Bull. **52**: 186–191.
30. Anzai, K., Furuse, M., Yoshida, A., Matsuyama, A., Moritake, T., Tsuboi, K. and Ikota, N. (2003) *In vivo* radioprotection of mice by 3-methyl-1-phenyl-2-pyrazolin-5-one (Edaravone; Radicut), a clinical drug. J. Radiat. Res. **45**: 319–323.
31. Peng, R., Wang, D., Wang, B., Xia, G., Li, Y., Xiong, C., Gao, Y., Yang, H. and Cui, Y. (1999) Apoptosis of hemopoietic cells in irradiated mouse bone marrow. J. Environ. Pathol. Toxicol. Oncol. **18**: 305–308.
32. Nakano, H., Kohara, M. and Shinohara, K. (2001) Evaluation of the relative contribution of p53-mediated pathway in X-ray-induced apoptosis in human leukemic MOLT-4 cells by transfection with a mutant p53 gene at different expression levels. Cell Tissue Res. **306**: 101–106.
33. Morita, A., Suzuki, N., Matsumoto, Y., Hirano, K., Enomoto, A., Zhu, J. and Sakai, K. (2000) p41 as a possible marker for cell death is generated by caspase cleavage of p42/SET β in irradiated MOLT-4 cells. Biochem. Biophys. Res. Commun. **278**: 627–632.
34. Enomoto, A., Suzuki, N., Hirano, K., Matsumoto, Y., Morita, A., Sakai, K. and Koyama, H. (2000) Involvement of SAPK/

JNK pathway in X-ray-induced rapid cell death of human T-cell leukemia cell line MOLT-4. Cancer Lett. **155**: 137–144.
35. Enomoto, A., Suzuki, N., Kang, Y., Hirano, K., Matsumoto, Y., Zhu, J., Morita, A., Hosoi, Y., Sakai, K. and Koyama, H. (2003) Decreased *c*-Myc expression and its involvement in X-ray-induced apoptotic cell death of human T-cell leukemia cell line MOLT-4. Int. J. Radiat. Biol. **79**: 589–600.
36. Nakano, H., Yonekawa, H. and Shinohara, K. (2003) Delayed expression of apoptosis in X-irradiated human leukemic MOLT-4 cells transfected with mutant p53. J. Radiat. Res. (Tokyo) **44**: 179–183.
37. Shinohara, K. and Nakano, H. (1993) Interphase death and reproductive death in X-irradiated MOLT-4 cells. Radiat. Res. **135**: 197–205.
38. Nishikawa, T., Edelstein, D., Du, X. L., Yamagishi, S., Matsumura, T., Kaneda, Y., Yorek, M. A., Beebe, D., Oates, P. J., Hammes, H. P., Giardino, I. and Brownlee, M. (2000) Normalizing mitochondrial superoxide production blocks three pathways of hyperglycaemic damage. Nature. **404**: 787–790.
39. Nagata, S. (2000) Apoptotic DNA fragmentation. Exp. Cell Res. **256**: 12–18.
40. Akagi, Y., Ito, K. and Sawada, S. (1993) Radiation induced apoptosis and necrosis in Molt-4 cells: a study of dose effect relationships and their modification. Int. J. Radiat. Biol. **64**: 47–56.
41. Cui, Z. G., Kondo, T., Feril, Jr. L. B., Waki, K., Inanami, O. and Kuwabara, M. (2004) Effects of antioxidants on X-ray- or hyperthermia- induced apoptosis in human lymphoma U937 cells. Apoptosis **9**: 757–763.
42. Salganik, R. I. (2001) The benefits and hazards of antioxidants: Controlling apoptosis and other protective mechanisms in cancer patients and the human population. J. Am. Coll. Nutr. **20**: 464S–472S.
43. Wahl, G. M. and Carr, A. M. (2001) The evolution of diverse biological responses to DNA damage: insights from yeast and p53. Nature Cell Biol. **3**: E277–E286.
44. Crosby, M. E., Oancea, M. and Almasan, A. (2004) p53 binding to target sites is dynamically regulated before and after ionizing radiation-mediated DNA damage. J. Environ. Pathol. Toxicol. Oncol. **23**: 67–79.
45. Morita, A., Zhu, J., Suzuki, N., Enomoto, A., Matsumoto, Y., Tomita, M., Suzuki, T., Ohtomo, K. and Hosoi, Y. (2006) Sodium orthovanadate suppresses DNA damage-induced caspase activation and apoptosis by inactivating p53. Cell Death Differ. **341**: 499–511.
46. Zheng, T. S., Hunot, S., Kuida, K. and Flavell, R. A. (1999) Caspase knockouts: matters of life and death. Cell Death Differ. **6**: 402–411.
47. Nicholson, D. W. (1999) Caspase structure, proteolytic substrates, and function during apoptotic cell death. Cell Death Differ. **6**: 1028–1042.
48. Gross, A., McDonnell, J. M. and Korsmeyer, S. J. (1999) BCL-2 family members and the mitochondria in apoptosis. Genes. Dev. **13**: 1899–1911.
49. Cheng, E. H., Kirsch, D. G., Clem, R. J., Ravi, R., Kastan, M. B., Bedi, A., Ueno, K. and Hardwick, J. M. (1997) Conversion of Bcl-2 to a Bax-like death effector by caspases. Science **278**: 1966–1968.
50. Rajesh, K. G., Sasaguri, S., Suzuki, R. and Maeda, H. (2003) Antioxidant MCI-186 inhibits mitochondrial permeability transition pore and upregulates Bcl-2 expression. Am. J. Physiol. Heart Circ. Physiol. **285**: H2171–H2178.
51. Song, Y., Li, M., Li, J. C. and Wei, E. Q. (2006) Edaravone protects PC12 cells from ischemic like injury via attenuating the damage to mitochondria. J. Zhejiang Univ. Sci. B **7**: 749–756.
52. Mantovani, G., Maccio, A., Madeddu, C., Mura, L., Gramignano, G., Russo, M. R., Murgia, V., Camboni, P., Ferreli, L., Mocci, M. and Massa, E. (2003) The impact of different antioxidant agents alone or in combination on reactive oxygen species, antioxidant enzymes and cytokines in a series of advanced cancer patients at different sites: correlation with disease progression. Free Radic. Res. **37**: 213–223.
53. McClain, D. E., Kalinich, J. F. and Ramakrishnan, N. (1995) Trolox inhibits apoptosis in irradiated MOLT-4 lymphocytes. FASEB J. **9**: 1345–1354.
54. Inanami, O., Takahashi, K. and Kuwabara, M. (1999) Attenuation of caspase-3-dependent apoptosis by Trolox post-treatment of X-irradiated MOLT-4 cells. Int. J. Radiat. Biol. **75**: 155–163.
55. Zhang, N., Komine-Kobayashi, M., Tanaka, R., Liu, M., Mizuno, Y. and Urabe, T. (2005) Edaravone reduces early accumulation of oxidative products and sequential inflammatory responses after transient focal ischemia in mice brain. Stroke. **36**: 2220–2225.
56. Yagi, Y., Horinaka, S. and Matsuoka, H. (2005) Edaravone prevented deteriorated cardiac function after myocardial ischemia-reperfusion via inhibiting lipid peroxidation in rat. J. Cardiovasc. Pharmacol. **46**: 46–51.
57. Marzatico, F., Porta, C., Moroni, M., Bertorelli, L., Borasio, E., Finotti, N., Pansarasa, O. and Castagna, L. (2000) *In vitro* antioxidant properties of amifostine (WR-2721, Ethyol). Cancer Chemother. Pharmacol. **45**: 172–176.
58. Grdina, D. J., Kataoka, Y., Basic, I. and Perrin, J. (1992) The radioprotector WR-2721 reduces neutron-induced mutations at the hypoxanthine-guanine phosphoribosyl transferase locus in mouse splenocytes when administered prior to or following irradiation. Carcinogenesis **13**: 811–814.

Received on May 24, 2007
Revision received on July 5, 2007
Accepted on August 3, 2007
J-STAGE Advance Publication Date: October 24, 2007

THE JOURNAL OF BIOLOGICAL CHEMISTRY VOL. 282, NO. 13, pp. 9895–9901, March 30, 2007

Functional Interaction between the Transcription Factor Krüppel-like Factor 5 and Poly(ADP-ribose) Polymerase-1 in Cardiovascular Apoptosis*

Received for publication, August 23, 2006, and in revised form, January 18, 2007 Published, JBC Papers in Press, February 5, 2007, DOI 10.1074/jbc.M608098200

Toru Suzuki[‡§1,2], **Toshiya Nishi**[‡1], **Tomoko Nagino**[‡1], **Kana Sasaki**[‡1], **Kenichi Aizawa**[‡], **Nanae Kada**[‡], **Daigo Sawaki**[‡], **Yoshiko Munemasa**[‡], **Takayoshi Matsumura**[‡], **Shinsuke Muto**[‡‖], **Masataka Sata**[‡], **Kiyoshi Miyagawa**[¶], **Masami Horikoshi**[‖], **and Ryozo Nagai**[‡3]

From the Departments of ‡Cardiovascular Medicine, §Clinical Bioinformatics, ¶Radiation Biology, Graduate School of Medicine, and ‖Laboratory of Developmental Biology, Institute of Molecular and Cellular Biosciences, The University of Tokyo, 7-3-1 Hongo, Bunkyo-ku, Tokyo 113-8655, Japan

Krüppel-like factor 5 (KLF5) is a transcription factor important in regulation of the cardiovascular response to external stress. KLF5 regulates pathological cell growth, and its acetylation is important for this effect. Its mechanisms of action, however, are still unclear. Analysis in KLF5-deficient mice showed that KLF5 confers apoptotic resistance in vascular lesions. Mechanistic analysis further showed that it specifically interacts with poly(ADP-ribose) polymerase-1 (PARP-1), a nuclear enzyme important in DNA repair and apoptosis. KLF5 interacted with a proteolytic fragment of PARP-1, and acetylation of KLF5 under apoptotic conditions increased their affinity. Moreover, KLF5 wild-type (but not a non-acetylatable point mutant) inhibited apoptosis as induced by the PARP-1 fragment. Collectively, we have found that KLF5 regulates apoptosis and targets PARP-1, and further, for acetylation to regulate these effects. Our findings thus implicate functional interaction between the transcription factor KLF5 and PARP-1 in cardiovascular apoptosis.

The cardiovasculature adapts dynamically to metabolic and/or mechanical stresses (*i.e.* blood vessel remodeling in response to oxidative and hypertensive stress). Although this response initially compensates for the pathological stimulus, chronic and excessive load ultimately leads to decompensatory maladaptation, which is the underlying pathology of heart failure and atherosclerosis (1, 2).

The cellular mechanisms underlying cardiovascular adaptation processes are characterized by cellular hypertrophy and death. Previous studies have begun to clarify the molecular basis of the process centered on signaling pathways linking extracellular stimuli to intracellular processes characterized by the intracellular signaling cascade and downstream gene expression events, which include roles of transcription factors, such as NFAT (nuclear factor of activated T cells) through the calcineurin pathway and histone deacetylases in cardiac hypertrophy (3–6). We have recently shown that the transcription factor, Krüppel-like factor 5 (KLF5),[4] regulates the cardiovascular response to pathological stress (*e.g.* angiotensin II) by modulating atherosclerosis, angiogenesis, and cardiac hypertrophy (7–10).

Although the transcriptional and signaling networks regulating the cardiac adaptation response have begun to be unraveled, further investigation is needed to better understand the pathogenic roles of the involved factors and pathways. Regulation of cell death/survival, in particular, remains poorly understood. Here, we have shown that KLF5 inhibits cell death/apoptosis and that it functionally interacts with poly(ADP-ribose) polymerase-1 (PARP-1), a nuclear enzyme involved in the response to DNA damage (11).

MATERIALS AND METHODS

Cell Culture and Apoptotic Assays—3T3 and HeLa cells were grown in Dulbecco's modified Eagle's medium supplemented with 10% serum. Human umbilical vein-derived endothelial cells were cultured in EBM-2 medium with EGM-2 supplement (Clonetics). Stable transformant cell lines derived from 3T3 and HeLa cells (12) were maintained in Dulbecco's modified Eagle's medium/10% serum containing 50 μg/ml G418 (Sigma). For most cell death/survival experiments, cells were treated with 50 ng/ml recombinant tumor necrosis factor-α (TNF-α) (Peprotech) and/or 4 μM actinomycin D (Sigma). Analysis in human umbilical vein-derived endothelial cells was done following transfection of expression vectors. Caspase-3 was assayed with the caspase-3 assay system (Promega). Cleaved DNA was assayed with the Cell death detection assay kit ELISA (enzyme-linked immunosorbent assay; Roche Applied Science). TUNEL

* This study was supported by grants from the Ministry of Education, Culture, Sports, Science, and Technology; New Energy Development Organization; Ministry of Health, Labor, and Welfare; and Japan Science and Technology Corporation. The costs of publication of this article were defrayed in part by the payment of page charges. This article must therefore be hereby marked "*advertisement*" in accordance with 18 U.S.C. Section 1734 solely to indicate this fact.

[1] These authors contributed equally to this work.
[2] To whom correspondence may be addressed: Depts. of Cardiovascular Medicine and Clinical Bioinformatics, Graduate School of Medicine, The University of Tokyo, 7-3-1 Hongo, Bunkyo-ku, Tokyo, Japan 113-8655. Tel.: 81-3-3815-5411 (ext. 33117); Fax: 81-3-5800-8824; E-mail: torusuzu-tky@umin.ac.jp.
[3] To whom correspondence may be addressed: Dept. of Cardiovascular Medicine, Graduate School of Medicine. The University of Tokyo, 7-3-1 Hongo, Bunkyo-ku, Tokyo, Japan 113-8655. Tel.: 81-3-3815-5411 (ext. 33100); Fax: 81-3-3815-2087; E-mail: nagai-tky@umin.ac.jp.

[4] The abbreviations used are: KLF5, Krüppel-like factor 5; PARP-1, poly(ADP-ribose) polymerase-1; TNF, tumor necrosis factor; TUNEL, terminal deoxynucleotidyltransferase-mediated dUTP nick-end labeling; GST, glutathione S-transferase.

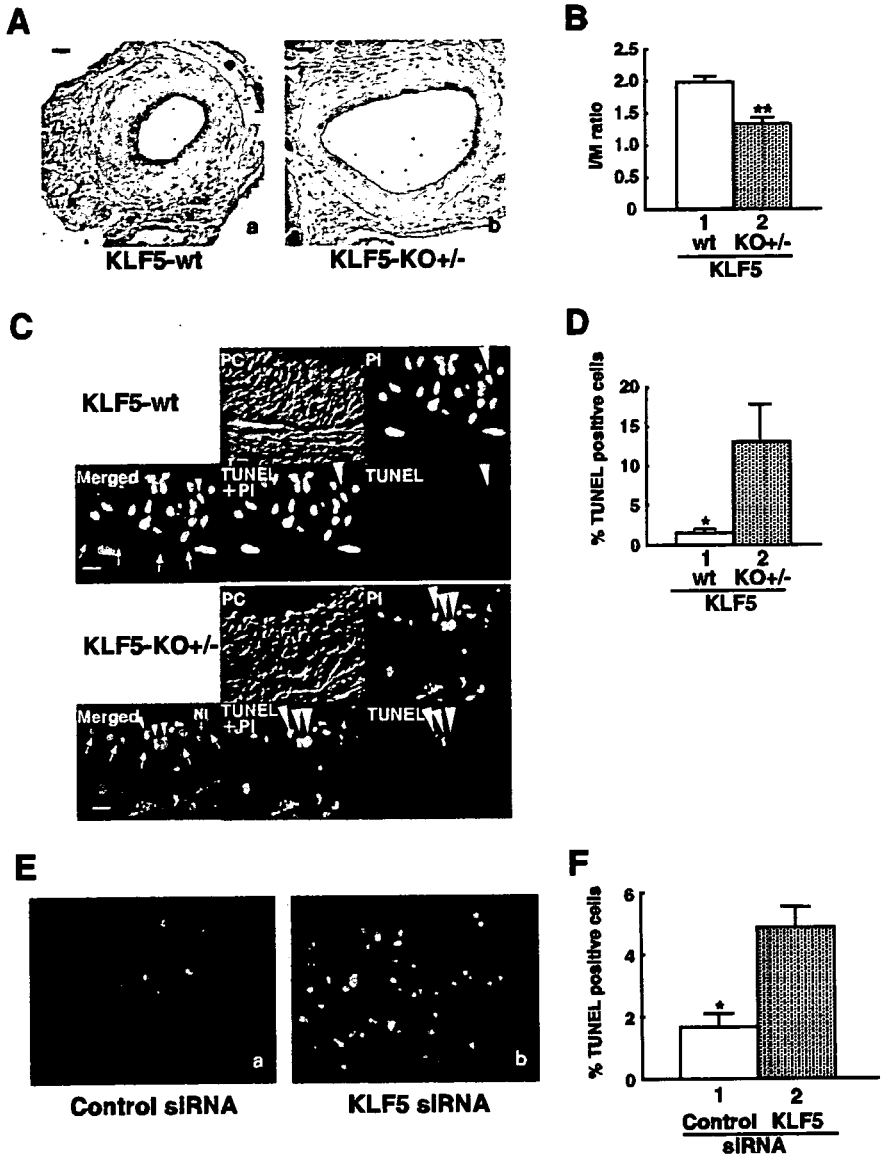

FIGURE 1. **Apoptotic resistance as a pathophysiological function of KLF5.** *A*, mouse femoral artery injury model in KLF5 wild type (*a*, *KLF5-wt*) and heterozygous knock-out (*b*, KLF5-KO$^{+/-}$) mice. Hematoxylin and eosin staining. *B*, intima to media (*I/M*) ratio ($n = 6$). *Error bars* represent S.E. *Scale bar*, 50 μm. **, $p < 0.01$. *C*, TUNEL staining of femoral artery injury samples. TUNEL is shown in *green* and propidium iodide (*PI*) in *red*. *Arrowheads* indicate merged TUNEL-positive nuclei (*yellow*). *Arrows* indicate the internal elastic lamina. *NI*, neointima; *PC*, phase contrast. *D*, graphical representation of TUNEL-positive apoptotic cells. *, $p < 0.05$. *E*, TUNEL staining in apoptotic cells subjected to RNA interference. HeLa cells were used on the basis that they contained the highest known endogenous levels of KLF5. *F*, graphical representation of TUNEL-positive apoptotic cells. *, $p < 0.05$.

staining was done with the *in situ* apoptosis detection kit (Takara) after cells were fixed with 4% paraformaldehyde. For the mouse femoral artery injury sections, the *in situ* death detection kit (Roche Applied Science) was used. Nuclei were counterstained with propidium iodide (Sigma). Sections were mounted with the ProLong antifade kit (Molecular Probes, Eugene, OR) and observed under a confocal microscope (Fluoview FV300; Olympus, Tokyo, Japan).

Mouse Femoral Artery Injury Model—Eight-week-old male KLF5 heterozygous knock-out mice (9) and wild-type littermates were subjected to femoral artery injury and analyzed as described previously (13).

RNA Interference Analysis—RNA interference analysis of KLF5 was done as described previously (14).

Immunoprecipitation and Western Blot Analysis—Whole cell lysate or nuclear extract was immunoprecipitated with anti-FLAG M2 affinity gel (Sigma), prepared anti-KLF5 antibody, or anti-PARP antibody (R & D Systems) with protein G-Sepharose (GE Healthcare), subjected to SDS-PAGE analysis, and then immunoblotted as described previously (12, 14). For Western blot analysis, antibodies from the apoptosis sampler kit (BD Biosciences) were used in addition to FLAG M2 monoclonal antibody (Sigma), anti-PARP-1 monoclonal antibody (BD Biosciences and R & D systems), anti-acetylated lysine antibody (Santa Cruz Biotechnology), and anti-KLF5 antibody (KM1785) (9). Plasmid transfections were done using Lipofectamine 2000 (Invitrogen). Adenoviral transfections were done as described previously (14).

Preparation of Anti-KLF5 Antibody—Anti-KLF5 antibody was prepared by immunizing rabbits with 100 μg of full-length purified recombinant His_6-KLF5 for 8 times at 1-week intervals, after which serum was extracted. Antibody specificity was confirmed by Western blot (data not shown).

Preparation of Recombinant Epitope-tagged Protein—Human KLF6 was PCR-amplified and subcloned into the pGEX vector (Amersham Biosciences). Expression and purification of bacterial recombinant proteins for GST-KLF6, KLF5, KLF5-K369R, zinc fingers, and His_6 24-kDa PARP-1 were done essentially as described previously (12, 15, 16).

Protein-Protein Interaction Assay and Acetylation Assay—Acetylation reactions and the GST pull down assay were done as previously described (12, 16).

Statistical Analysis—All data were analyzed by the non-paired *t* test. $p < 0.05$ was considered significant.

RESULTS

Apoptotic Resistance Is a Pathophysiological Function of KLF5—The present study began with the initial observation of an attenuated response to vascular injury in KLF5 knock-out mice subjected to a mouse femoral artery injury model (9) (Fig. 1, *A* and *B*). To understand the mechanisms underlying this effect on neointimal hyperplasia, we questioned whether cell

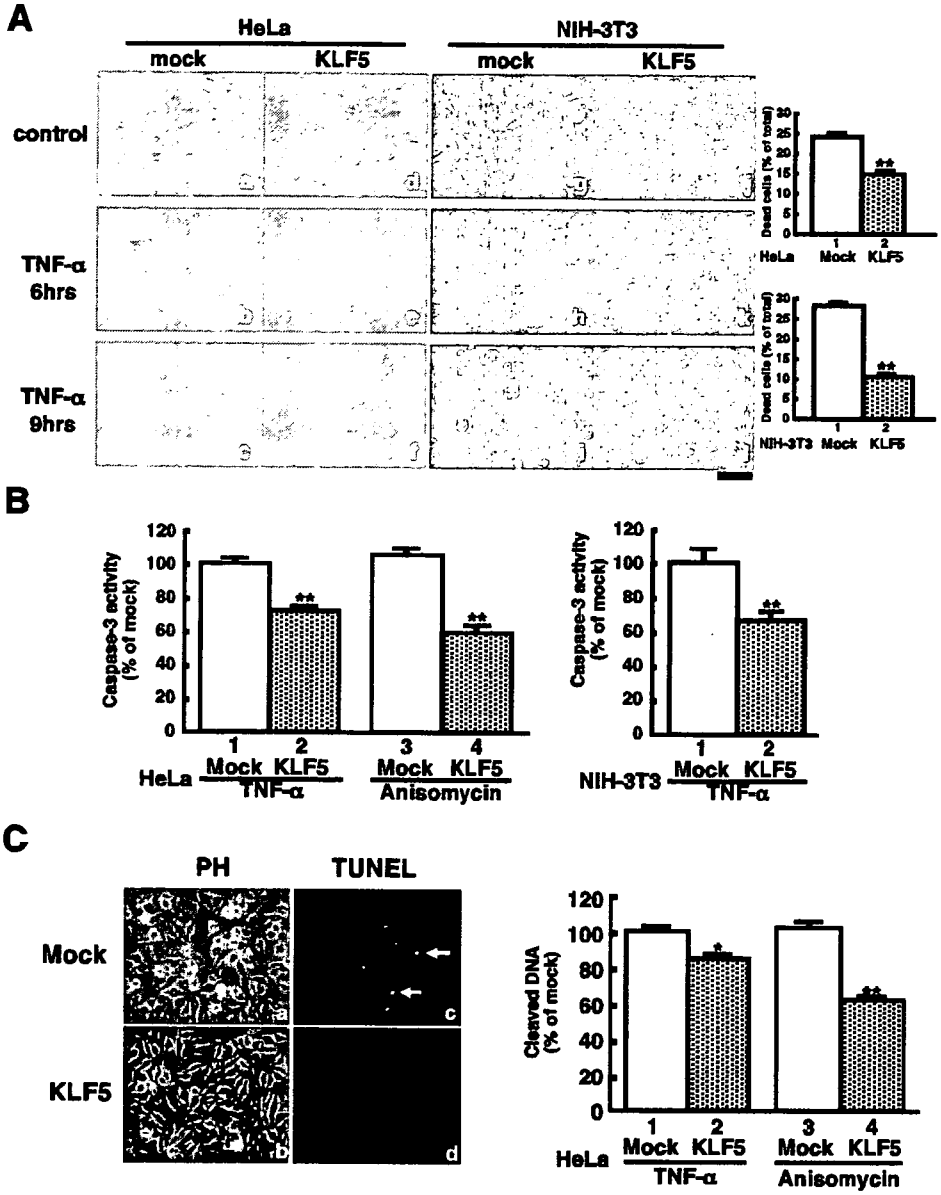

FIGURE 2. **Apoptotic resistance activity of KLF5 in cells.** *A*, phase contrast photomicrographs of mock vector (*HeLa, a–c; NIH-3T3, g–i*) and KLF5 stable transformants (*HeLa, d–f; NIH-3T3, j–l*) treated with TNF-α. The time course is as indicated. *Scale bar*, 100 μm. Quantification of cell survival shown on *right*. Results are presented as the percent of control. **, $p < 0.01$ *versus* mock. *B*, quantification of caspase-3 activity. Results are shown as the percent of the mock-transfected cell line. **, $p < 0.01$ *versus* mock. *C*, TUNEL staining of cells. Photomicrographs of cells examined by phase contrast (*PH*) microscopy (*a* and *b*) and fluorescence microscopy (*c* and *d*) are shown. Apoptotic cells are identified by their highly condensed or fragmented nuclei (*arrows* in *panel c*). Quantification of DNA fragmentation is shown on the *right*. Results are shown as the percent of the mock-transfected cell line. *, $p < 0.05$. *versus* mock; **, $p < 0.01$ *versus* mock.

death/apoptosis might play a pathological role, given that cellular apoptosis is a major mechanism of the wire injury model that was used (13). Analysis of apoptosis by TUNEL staining showed an increase in TUNEL-positive apoptotic cells in the neointima of knock-out mice as compared with wild-type littermates (13.1 *versus* 1.5%) (Fig. 1, *C* and *D*). Insufficiency of KLF5 therefore resulted in decreased neointima formation most likely due to enhanced apoptotic cell death after vascular injury.

To confirm that KLF5 insufficiency is associated with increased apoptosis at the cellular level, we next used an RNA interference approach to knockdown KLF5 under apoptotic stimulation (TNF-α). TUNEL staining showed an increase in positive staining cells when subjected to KLF5 small interfering RNA as compared with control small interfering RNA (secreted alkaline phosphatase) (Fig. 1, *E* and *F*). Thus, KLF5 insufficiency is associated with increased apoptosis.

Cellular Apoptotic Resistance of KLF5—To characterize the apoptotic resistance mechanisms of KLF5, stable transformants (cloned) expressing KLF5 in human HeLa and murine 3T3 cells were used for further investigations. Both KLF5-expressing cells showed resistance to induced cell death by TNF-α as compared with mock cells (Fig. 2*A*). We then measured apoptotic caspase-3 activity, which was reduced in both KLF5-expressing cells (29% for TNF-α stimulation and 44% for anisomycin treatment in HeLa cells and 34% in 3T3 cells for TNF-α stimulation) (Fig. 2*B*). Further, TUNEL staining showed that KLF5-expressing cells were resistant to DNA cleavage by apoptotic stimulation as shown by quantification of TUNEL-positive cells (15% by TNF-α and 40% by anisomycin) (Fig. 2*C*). Thus, cells expressing KLF5 were consistently resistant to apoptosis by criteria including morphology, caspase-3 activity, and DNA cleavage (TUNEL). Apoptotic resistance was confirmed in at least two independent clones for both HeLa and NIH3T3 cells as well as in a resistance-selected heterogenous noncloned colony (data not shown).

Mechanisms of Apoptosis-resistant Activity of KLF5—Next, to investigate the molecular mechanisms of the apoptosis-resistant effects of KLF5, the expression levels of a panel of proteins related to the apoptotic signaling cascade were examined in the HeLa stable transformant with apoptotic stimulation by TNF-α. Although there were no apparent effects on the expression of most of these apoptosis-related proteins, the protein level of poly(ADP-ribose) polymerase-1 (PARP-1) was markedly affected in KLF5-expressing cells as compared with the control (Fig. 3*A*). PARP-1 is a 113-kDa nuclear enzyme involved in DNA repair that catalyzes the initiation, elongation, and branching of poly(ADP-ribose) onto its target protein (11).

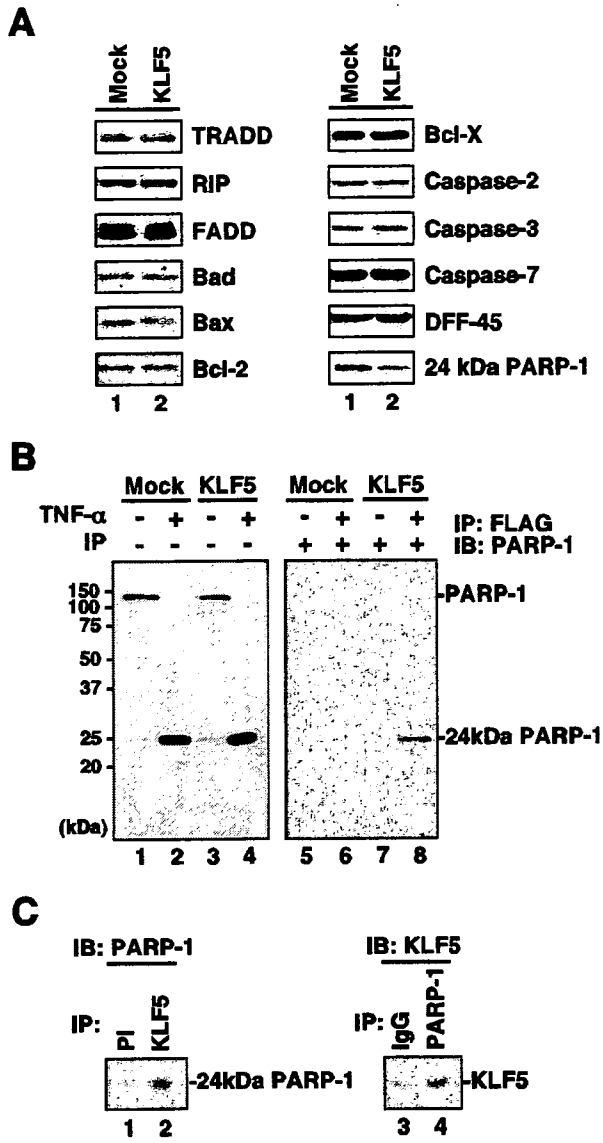

FIGURE 3. **Mechanisms of KLF5 apoptotic resistance activity and effects on PARP-1.** *A*, immunoblots of apoptosis-related proteins in KLF5-expressing cells subjected to TNF-α apoptotic stimulus. *TRADD*, TNF-R-associated death domain; *RIP*, receptor-interacting protein; *FADD*, Fas-associated death domain; *Bad*, Bcl-2 antagonist of cell death; *Bax*, Bcl-2-associated X protein; *Bcl-2*, B cell lymphoma/leukemia-2; *DFF-45*, 45-kDa DNA fragmentation factor; *PARP-1*, poly(ADP-ribose) polymerase-1. *B*, immunoprecipitation of apoptotic stimulus-induced 24-kDa pro-apoptotic fragment of PARP-1 by FLAG-tagged KLF5 *in vivo*. *Lanes 1–4* are whole cell lysate input. Protein amounts were normalized to show the difference in binding affinities. *IP*, immunoprecipitation; *IB*, immunoblot. *C*, immunoprecipitation of endogenous KLF5 and PARP-1 proteins in endothelial cells. Immunoprecipitation by anti-KLF5 antibody followed by immunoblot with anti-PARP-1 antibody using pre-immune serum (*PI*) as control is shown on the *left*, and the reverse experiment of immunoprecipitation by anti-PARP-1 antibody followed by immunoblot with anti-KLF5 (KM1785) antibody using IgG as control is shown on the *right*. Cells were treated with anisomycin.

PARP-1 is cleaved by caspase into a 24-kDa amino-terminal DNA-binding domain and an 89-kDa carboxyl-terminal catalytic domain under apoptotic conditions. This result was not unexpected, given that caspase cleaves PARP-1, and as caspase-3 activity was reduced in KLF5-expressing cells (Fig. 2*B*). RNA interference experiments confirmed involvement of PARP-1 in apoptosis of the tested HeLa cells (data not shown).

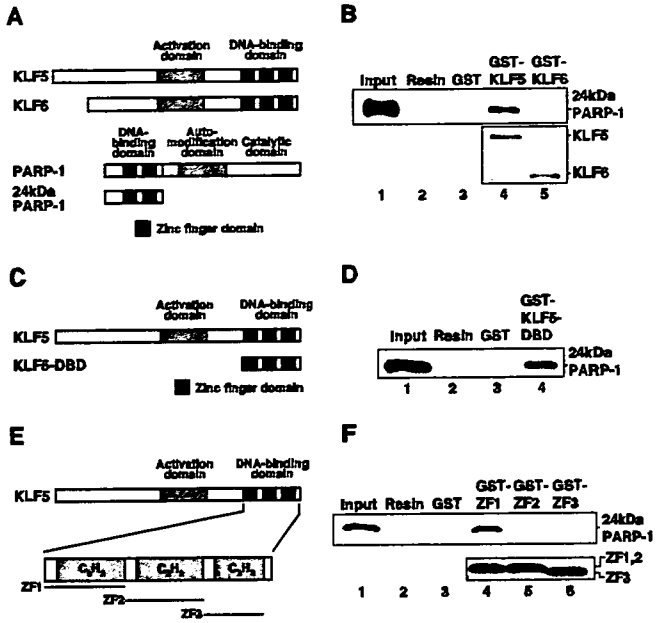

FIGURE 4. **Specific interaction between apoptotic resistant KLF5 and 24 kDa PARP-1 *in vitro*.** *A*, Schematic representation of KLF5, KLF6 and PARP-1. *B*, GST pulldown assay of KLF5 and KLF6 with the 24 kDa pro-apoptotic fragment of PARP-1. *C*, Schematic representation of full-length KLF5 and DNA-binding domain (DBD) of KLF5. *D*, GST pulldown assay of KLF5 DNA-binding domain (DBD) and the 24 kDa pro-apoptotic fragment of PARP-1. *E*, Schematic representation of KLF5 zinc finger peptide motifs. *F*, GST pulldown assay of KLF5 zinc finger peptides and the 24 kDa pro-apoptotic fragment of PARP-1.

Nevertheless, we further pursued actions of KLF5 on PARP-1 under apoptotic conditions given the specific effects on PARP-1. We hypothesized that PARP-1 and KLF5 might functionally interact, given that they are zinc finger proteins that often physically and functionally interact (17). Immunoprecipitation experiments showed that KLF5 interacts with PARP-1, and strikingly, for this interaction to be specific with the 24-kDa fragment under apoptotic conditions (Fig. 3*B*). Note that loading amounts of protein were normalized to show the difference in binding affinities. KLF5 did not interact with the 89-kDa carboxyl-terminal catalytic domain under these conditions (data not shown).

As these experiments were done using the stable transformant, further immunoprecipitation experiments were done to confirm interaction by endogenous proteins (Fig. 3*C*). Immunoprecipitation experiments using anti-KLF5 and PARP-1 antibodies confirmed that KLF5 and the PARP-1 24-kDa fragment interact in the cell. We thus sought to understand the functional implications and regulation of this interaction.

Interaction between KLF5 and PARP-1—To characterize the interaction between KLF5 and PARP-1, we next examined the specificity and site of interaction. For specificity, we compared the binding of PARP-1 between KLF5 and KLF6, the latter being a similar Krüppel-like factor (18, 19) (Fig. 4, *A* and *B*). GST pulldown assay under conditions in which KLF5 bound the 24-kDa fragment of PARP-1 (Fig. 4*B*, *lane 4*) showed a lack of interaction with KLF6 (Fig. 4*B*, *lane 5*). Thus, interaction of KLF5 with PARP-1 was direct and specific.

We further determined the site of interaction between KLF5 and PARP-1. To confirm our initial expectations that the zinc

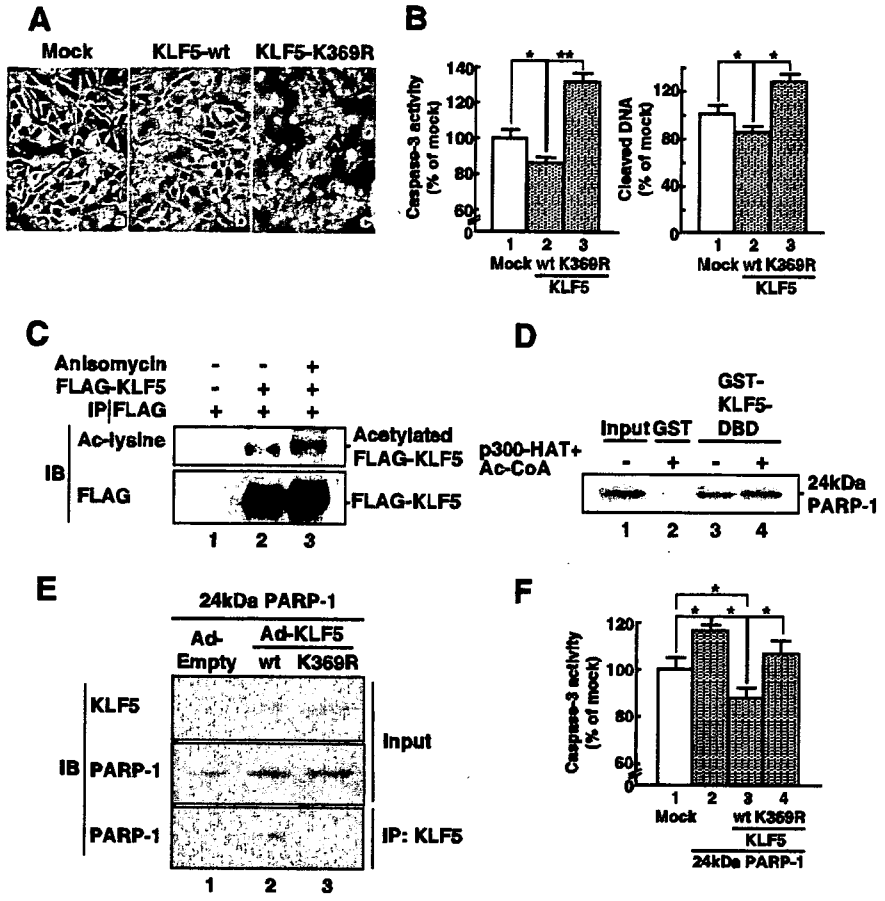

FIGURE 5. **Effect of acetylation on KLF5 apoptotic resistance and interaction with PARP-1.** *A, B,* Effect of non-acetylatable point mutant of KLF5 (K369R) on apoptotic resistance. K369R is a lysine (K) to arginine (R) mutation at the 369th amino acid residue of KLF5. Morphological assessment by phase contrast microscopy (A) and quantification of caspase-3 activity and DNA cleavage (B). Results are shown as percent change of mock transfected cell line. *, $p < 0.05$; **, $p < 0.01$. *C,* Western blot analysis with anti-acetylated lysine-antibody under cellular apoptotic conditions. *D,* Effect of acetylation on interaction of KLF5 and PARP-1. Protein-protein interaction assayed using *in vitro* acetylated recombinant KLF5. *E,* Co-immunoprecipitation of the 24 kDa pro-apoptotic fragment of PARP-1 with wild-type KLF5 and point mutant KLF5-K369R. *F,* Effects of KLF5 wild-type and K369R mutant on apoptosis as induced by the 24 kDa pro-apoptotic fragment of PARP-1 in endothelial cells. *, $p < 0.05$ *versus* mock.

finger motif is the protein-protein interaction interface (12, 17), we tested whether the zinc finger 24-kDa fragment of PARP-1 directly interacts with the zinc finger DNA-binding domain of KLF5 (Fig. 4, *C* and *D*). The GST pulldown assay showed that the zinc finger region of KLF5 directly and specifically bound the 24-kDa fragment of PARP-1 (Fig. 4*D*, *lane 4*). Given that the zinc finger regions of KLF5 and PARP-1 (which mediate their interaction) comprise their DNA-binding domains, we tested the requirement of DNA by competitively adding DNA to protein interaction assays, which showed that DNA is not necessary for this interaction and for this interaction to thus be mediated by protein-protein interaction (data not shown).

As the zinc finger DNA-binding domain of KLF5 contains three zinc finger motifs, we next examined whether there is specific binding of individual zinc fingers to PARP-1 (Fig. 4*E*). The GST pulldown assay showed the first zinc finger but not the second nor third zinc finger peptides to interact with PARP-1 (Fig. 4*F*, *lanes 4–6*).

Acetylation Is Important for the Apoptosis-resistant Effects of KLF5—As the interaction with PARP-1 was mediated through the first zinc finger of KLF5 (Fig. 4*F*) (which contains a lysine residue whose acetylation we have previously shown to be important for the cell growth stimulatory effects of KLF5 (12)), we next asked whether acetylation is important for apoptosis-resistant actions and interaction with PARP-1.

First, we examined whether a non-acetylatable point mutant of KLF5 (K369R, lysine → arginine substitution at residue 369) would lack resistance to apoptosis. Stable transformants in 3T3 cells of wild type and that of the point mutant K369R of KLF5 were subjected to apoptotic stimulus (TNF-α), and morphology was examined in addition to quantification of caspase-3 activity and DNA cleavage. As compared with wild-type KLF5-expressing cells, cells expressing the point mutant KLF5-K369R were less viable in response to apoptotic stimulus (TNF-α)(Fig. 5, *A* and *B*). Caspase-3 and DNA cleavage assay both showed that the point mutant KLF5-K369R did not inhibit apoptosis under conditions in which KLF5 wild type showed significant inhibition. Adenoviral transfer of the wild type and point mutant K369R into balloon-injured rat cartotid arteries confirmed that the wild type but not the point mutant K369R can inhibit pathophysiological vascular apoptosis.[5] These findings suggest acetylation of KLF5 is important for its apoptosis-resistant cellular effects.

The former experiments suggested that KLF5 is likely acetylated under apoptotic conditions. To test this, Western blot analysis using antibody against acetylated lysine was done that showed KLF5 is markedly acetylated under apoptotic conditions (Fig. 5*C*, *lane 3*)), although we did see some acetylation under basal conditions (*lane 2*). We next asked whether acetylation might regulate interaction between KLF5 and the PARP-1 fragment. A protein-protein interaction assay using *in vitro* acetylated KLF5 was done that showed acetylation of KLF5 increased its binding affinity with the PARP-1 fragment (Fig. 5*D*, *lane 4 versus lane 3*), although we did note that the addition of the p300 acetyltransferase region alone resulted in a

[5] D. Sawaki, T. Suzuki, and R. Nagai, unpublished data.

marginal increase (data not shown). We further examined whether acetylation augments interaction between KLF5 and the PARP-1 fragment in the cell. Immunoprecipitation experiments in endothelial cells transfected by adenovirus expressing similar amounts of wild-type or the point mutant KLF5-K369R followed by immunoprecipitation of similar amounts of the 24-kDa PARP-1 fragment by anti-PARP-1 antibody showed that wild-type KLF5 but not the point mutant KLF5-K369R to selectively interact with the PARP-1 24-kDa fragment (Fig. 5*E*, *lane 2 versus lane 3*). Acetylation of KLF5 is thus induced under apoptotic conditions and is important for its apoptosis-resistant activity as well as its interaction with PARP-1.

We further characterized the functional effects of this selective interaction. We reasoned that wild-type but not the point mutant KLF5-K369R may inhibit apoptosis induced by the 24-kDa pro-apoptotic fragment of PARP-1 (16, 20). The 24-kDa pro-apoptotic fragment of PARP-1 and wild-type KLF5 or the point mutant KLF5-K369R were transfected into endothelial cells, and effects on apoptosis were determined by examining caspase-3 activity. Under conditions in which the 24-kDa pro-apoptotic fragment of PARP-1 stimulated apoptosis, although marginally in our hands (Fig. 5*F*, *lane 1 versus lane 2*), wild-type KLF5 inhibited caspase-3 activity in contrast to the point mutant KLF5-K369R in which suppression of caspase-3 activity was not seen (Fig. 5*F*, *lane 3 versus lane 4*). These experiments showed that wild-type KLF5 but not the point mutant KLF5-K369R can inhibit apoptotic activity as stimulated by overexpression of the 24-kDa pro-apoptotic fragment of PARP-1.

DISCUSSION

Functional Interaction between KLF5 and PARP-1—The cardiovascular transcription factor, Krüppel-like factor 5 (KLF5), inhibits cell death/apoptosis and functionally interacts with PARP-1, a highly abundant nuclear enzyme that functions as a sensor of DNA damage. To our knowledge, KLF5 is the first protein to interact specifically and functionally with the 24-kDa PARP-1 fragment. This PARP-1 fragment also, at least partially, mediates physical interaction with the Werner syndrome protein and also likely with DNA ligase III (21, 22), but neither the specificity nor the functional effect of the interaction had been addressed.

The PARP-1 fragment has been reported to harbor pro-apoptotic activity (16). We have found that KLF5 is able to inhibit the marginal pro-apoptotic effects of the PARP-1 fragment, that KLF5 interacts with this peptide, and that acetylation of KLF5 stimulates this interaction. It is tempting to speculate that sequestration of the PARP-1 proteolytic fragment by KLF5 may be a novel target for regulation of PARP-1 actions.

However, we do note that the effects of PARP-1 on apoptosis remain controversial. Gene ablation studies in mice have shown that PARP-1 is not essential for apoptosis (23, 24). Additionally, cells exhibiting cleaved PARP-1 can divide normally (25), making its instructive role in apoptosis unclear. The fragment being produced after the apoptotic commitment step of caspase activation makes it further unlikely to be a critical determinant of apoptotic progression. Further investigation of the functional effect of the interaction with KLF5 will require a better understanding on the precise role of the PARP-1 fragment.

Regulatory Effects of Acetylation—Another important finding of the present study is that the signaling modification (acetylation) was shown to play an important role in the effects of KLF5 on cell death and interaction with PARP-1. Acetylation is a nucleus specific signaling modification that affects protein-protein as well as protein-DNA interactions by various nuclear factors (*e.g.* Armadillo and T-cell factor, Importin α and β) (26, 27). Although the biological role of this modification is not well understood, we show that it affects multiple activities of KLF5.

A recent study showed that acetylation of Sp1, a close relative of KLF5 that we previously showed to be acetylated (28–30), can be similarly induced by an apoptosis-inducing anti-cancer agent (31), which together with our findings may suggest that acetylation plays a key role in regulation of cell death/survival pathways in this family of factors. Further, as deacetylase (6) as well as acetylase and its activity (32) have been implicated in the cardiovascular remodeling response in the heart, this signaling pathway may have general implications for regulating the cardiovascular cell phenotype in response to pathological stress. KLF5, therefore, through acting on apoptotic pathways, may tip the balance between survival/repair and death/apoptosis under cardiovascular pathophysiological settings.

Acknowledgment—We thank Dr. M. Satoh for PARP-1 constructs.

REFERENCES

1. Olson, E. N. (2004) *Nat. Med.* **10,** 467–474
2. Towbin, J. A., and Bowles, N. E. (2002) *Nature* **415,** 227–233
3. Molkentin, J. D., Lu, J. R., Antos, C. L., Markham, B., Richardson, J., Robbins, J., Grant, S. R., and Olson, E. N. (1998) *Cell* **93,** 215–228
4. Molkentin, J. D., and Dorn, I. G., II (2001) *Annu. Rev. Physiol.* **63,** 391–426
5. Sussman, M. A., Lim, H. W., Gude, N., Taigen, T., Olson, E. N., Robbins, J., Colbert, M. C., Gualberto, A., Wieczorek, D. F., and Molkentin, J. D. (1998) *Science* **281,** 1690–1693
6. Zhang, C. L., McKinsey, T. A., Chang, S., Antos, C. L., Hill, J. A. and Olson, E. N. (2002) *Cell* **110,** 479–488
7. Hoshino, Y., Kurabayashi, M., Kanda, T., Hasegawa, A., Sakamoto, H., Okamoto, E., Kowase, K., Watanabe, N., Manabe, I., Suzuki, T., Nakano, A., Takase, S., Wilcox, J. N., and Nagai, R. (2000) *Circulation* **102,** 2528–2534
8. Shi, H., Zhang, Z., Wang, X., Liu, S., and Teng, C. T. (1999) *Nucleic Acids Res.* **27,** 4807–4815
9. Shindo, T., Manabe, I., Fukushima, Y., Tobe, K., Aizawa, K., Miyamoto, S., Kawai-Kowase, K., Moriyama, N., Imai, Y., Kawakami, H., Nishimatsu, H., Ishikawa, T., Suzuki, T., Morita, H., Maemura, K., Sata, M., Hirata, Y., Komukai, M., Kagechika, H., Kadowaki, T., Kurabayashi, M., and Nagai, R. (2002) *Nat. Med.* **8,** 856–863
10. Watanabe, N., Kurabayashi, M., Shimomura, Y., Kawai-Kowase, K., Hoshino, Y., Manabe, I., Watanabe, M., Aikawa, M., Kuro-o, M., Suzuki, T., Yazaki, Y., and Nagai, R. (1999) *Circ. Res.* **85,**182–191
11. D'Amours, D., Desnoyers, S., D'Silva, I., and Poirier, G. G. (1999) *Biochem. J.* **342,** 249–268
12. Miyamoto, S., Suzuki, T., Muto, S., Aizawa, K., Kimura, A., Mizuno, Y., Nagino, T., Imai, Y., Adachi, N., Horikoshi, M., and Nagai, R. (2003) *Mol. Cell. Biol.* **23,** 8528–8541
13. Sata, M., Maejima, Y., Adachi, F., Fukino, K., Saiura, A., Sugiura, S., Aoyagi, T., Imai, Y., Kurihara, H., Kimura, K., Omata, M., Makuuchi, M., Hirata, Y., and Nagai, R. (2000) *J. Mol. Cell. Cardiol.* **32,** 2097–2104
14. Aizawa, K., Suzuki, T., Kada, N., Ishihara, A., Kawai-Kowase, K.,

Matsumura, T., Sasaki, K., Munemasa, Y., Manabe, I., Kurabayashi, M., and Nagai, R. (2004) *J. Biol. Chem.* **279,** 70–76
15. Suzuki, T., Kimura, A., Nagai, R., and Horikoshi, M. (2000) *Genes Cells* **5,** 29–41
16. Yung, T. M. C., and Satoh, M. S. (2001) *J. Biol. Chem.* **276,** 11279–11286
17. Mackay, J. P., and Crossley, M. (1998) *Trends Biochem. Sci.* **23,** 1–4
18. Narla, G., Heath, K. E., Reeves, H. L., Li, D., Giono, L. E., Kimmelman, A. C., Glucksman, M. J., Narla, J., Eng, F. J., Chan, A. M., Ferrari, A. C., Martignetti, J. A., and Friedman, S. L. (2001) *Science* **294,** 2563–2566
19. Suzuki, T., Yamamoto, T., Kurabayashi, M., Nagai, R., Yazaki, Y., and Horikoshi, M. (1998) *J. Biochem.* **124,** 389–395
20. Kim, J. W., Won, J., Sohn, S., and Joe, C. O. (2000) *J. Cell Sci.* **113,** 55–961
21. Schreiber, V., Amé, J. C., Dollé, P., Schultz, I., Rinaldi, B., Fraulob, V., Ménissier-de Murcia, J., and de Murcia, G. (2002) *J. Biol. Chem.* **277,** 23028–23036
22. von Kobbe, C., Harrigan, J. A., Schreiber, V., Stiegler, P., Piotrowski, J., Dawut, L., and Bohr, V. A. (2004) *Nucleic Acids Res.* **32,** 4003–4014
23. De Murcia, J. M., Niedergang, C., Trucco, C., Ricoul, M., Dutrillaux, B., Mark, M., Oliver, F. J., Masson, M., Dierich, A., Le Meur, M., Walztinger, C., Chambon, P., and de Murcia, G. (1997) *Proc. Natl. Acad. Sci. U. S. A.* **94,** 7303–7307
24. Wang, Z. Q., Stingl, L., Morrison, C., Jantsch, M., Los, M., Schulze-Osthoff, K., and Wagner, E. F. (1997) *Genes Dev.* **11,** 2347–2358
25. Yang, L., Cao, Z., Yan, H., and Wood, W. C. (2003) *Cancer Res.* **63,** 6815–6824
26. Bannister, A. J., Miska, E. A., Gorlich, D., and Kouzarides, T., (2000) *Curr. Biol.* **10,** 467–470
27. Waltzer, L., and Bienz, M. (1998) *Nature* **395,** 521–525
28. Suzuki, T., Muto, S., Miyamoto, S., Aizawa, K., Horikoshi, M., and Nagai, R. (2003) *J. Biol. Chem.* **278,** 28758–28764
29. Suzuki, T., Aizawa, K., Matsumura, T., and Nagai, R. (2005) *Arterioscler. Thromb. Vasc. Biol.* **25,** 1135–1141
30. Suzuki, T., Matsumura, T., and Nagai, R. (2005) *Trends Cardiovasc. Med.* **15,** 125–129
31. Torigoe, T., Izumi, H., Wakasugi, T., Niina, I., Igarashi, T., Yoshida, T., Shibuya, I., Chijiiwa, K., Matsuo, K., Itoh, H., and Kohno, K., (2005) *J. Biol. Chem.* **280,** 1179–1185
32. Miyamoto, S., Kawamura T., Morimoto, T., Ono, K., Wada, H., Kawase, Y., Matsumori, A., Nishio, R., Kita, T., and Hasegawa, K. (2006) *Circulation* **113,** 679–690